

# Archosauriform footprints in the Lower Triassic of Western Alps and their role in understanding the effects of the Permian-Triassic hyperthermal

Fabio M. Petti $^1$ , Heinz Furrer $^2$ , Enrico Collo $^3$ , Edoardo Martinetto $^4$ , Massimo Bernardi $^1$ , Massimo Delfino $^4$ , Marco Romano  $^{\text{Corresp.},5}$ , Michele Piazza $^6$ 

<sup>1</sup> MUSE - Museo delle Scienze, Trento, Trento, Italy

<sup>2</sup> Paläontologisches Institut und Museum, Universität Zürich, <mark>Zürich,</mark> Switzerland

Natura Occitana, Dronero (CN), Dronero (CN), Italy

<sup>4</sup> Dipartimento di Scienze della Terra, Università degli Studi di Torino, Torin, Italy

Scienze della Terra, University of Roma "La Sapienza", Rome, Italy

<sup>6</sup> Dipartimento di Scienze della Terra, dell'Ambiente e della Vita, Università di Genova, Genoa, Italy

Corresponding Author: Marco Romano Email address: marco.romano@uniroma1.it

The most accepted killing model for the Permian-Triassic mass extinction (PTME) postulates that massive volcanic eruption (i.e. the Siberian Traps LIP) to geologically rapid global warming, acid rain and ocean anoxia. On land, habitable zones were drastically reduced, due to the combined effects of heating, drought and acid rains. This hyperthermal had severe effects also on the paleobiogeography of several groups of organisms. Among those, the tetrapods, whose geographical distribution across the end-Permian mass extinction (EPME) was the subject of controversy of a number precent papers. We here describe and interpret a new Early Triassic (?Olenekian) archosaur track assemblage from the Gardetta Plateau (Briançonnais, Western Alps, Italy) which, at the Permian-Triassic boundary, was placed at about 11° North. The tracks, both arranged in trackways and documented by single, well-preserved imprints, are assigned to Isochirotherium gardettae ichnosp. nov., and are here interpreted as produced by a nonarchosaurian archosauriform (erytrosuchid?) trackmaker. This new discovery provides further evidence for the presence of archosauriformes at low latitudes during the Early Triassic epoch, supporting a model in which the PTME did not completely vacate lowlatitude lands from tetrapods that therefore would have been able to cope with the extreme hot temperatures of Pangaea mainland.



1	Archosauriform footprints in the Lower Triassic of Western Alps and their
2	role in understanding the effects of the Permian-Triassic hyperthermal
3	
4	Fabio M. Petti <sup>1</sup> , Heinz Furrer <sup>2</sup> , Enrico Collo <sup>3</sup> ,
5	Edoardo Martinetto <sup>4</sup> , Massimo Bernardi <sup>1</sup> , Massimo Delfino <sup>4</sup> , Marco Romano <sup>5,*</sup>
6	and Michele Piazza <sup>6</sup>
7	
8	<sup>1</sup> MUSE – Museo delle Scienze, Trento
9	<sup>2</sup> Paläontologisches Institut und Museum, Universität Zürich, Zürich
10	<sup>3</sup> Natura Occitana, Dronero (CN)
11	<sup>4</sup> Dipartimento di Scienze della Terra, Università degli Studi di Torino, Torino
12	<sup>5</sup> Dipartimento di Scienze della Terra, Sapienza Università di Roma, Roma
13	<sup>6</sup> Dipartimento di Scienze della Terra, dell'Ambiente e della Vita, Università di Genova, Genova
14	
15	*Corresponding author e-mail: marco.romano@uniroma1.it
16	
17	Key words: Isochirotherium gardettae n. ichnosp., climate warming, extinction, Lower Triassic,
18	Italy.
19	
20	
21	
22	



_	$\overline{}$
•	~

# ABSTRACT

The most accepted killing model for the Permian-Triassic mass extinction (PTME) postulates
that massive volcanic eruption (i.e. the Siberian Traps LIP) led to geologically rapid global
warming, acid rain and ocean anoxia. On land, habitable zones were drastically reduced, due to
the combined effects of heating, drought and acid rains. This hyperthermal had severe effects
also on the paleobiogeography of several groups of organisms. Among those, the tetrapods,
whose geographical distribution across the end-Permian mass extinction (EPME) was the subject
of controversy of a number of recent papers. We here describe and interpret a new Early Triassic
(?Olenekian) archosaur track assemblage from the Gardetta Plateau (Briançonnais, Western
Alps, Italy) which, at the Permian-Triassic boundary, was placed at about 11° North. The tracks,
both arranged in trackways and documented by single, well-preserved imprints, are assigned to
Isochirotherium gardettae ichnosp. nov., and are here interpreted as produced by a non-
archosaurian archosauriform (erytrosuchid?) trackmaker. This new discovery provides further
evidence for the presence of archosauriformes at low latitudes during the Early Triassic epoch,
supporting a model in which the PTME did not completely vacate low-latitude lands from
tetrapods that therefore would have been able to cope with the extreme hot temperatures of
Pangaea mainland

# INTRODUCTION



15	The Permian-Triassic mass extinction (PTME) was the most severe biotic crisis of all times
16	(Erwin, 1993), eliminating > 90% of marine and terrestrial species (Erwin, 1993; Song et al.,
17	2013, 2015). After the mass extinction, totally new clades emerged, which include decapods and
18	marine reptiles in the oceans and new tetrapods on land (Chen and Benton, 2012). In the last
19	decade different physical environmental shocks have been identified as possible triggers for the
50	huge crisis, which include increased atmospheric CO <sub>2</sub> concentrations, global warming, acid rain,
51	ocean anoxia, ocean acidification and hypercapnia (Chen and Benton, 2012; Benton, 2018). The
52	most accepted killing model (e.g. Benton & Twitchett, 2003; Chen & Benton, 2012; Benton &
53	Newell, 2014; Shen et al., 2019) postulates an initial megascale eruption (more than 1,000
54	Gigatonnes of erupted lava, see Grasby et al., 2011), that released consistent amount of sulphate
55	aerosols and methane from clathrate reservoirs (see Berner, 2002), which led to global warming
56	and acid rain, causing a generalized plant die-offs and thus intensive erosion of the soil (Wignall,
57	2001; Benton, 2003, 2018; Benton & Twitchett, 2003; Sephton et al., 2005; Knoll et al., 2007).
58	On land, habitable zones were drastically reduced, due to the combination of extreme heat,
59	drought and acid rains, which caused progressive loss of soil and forests and had direct impact
50	on lacustrine organisms and any land-dwelling animal (Benton & Newell, 2014).
51	According to several authors (Joachimski et al., 2012; Sun et al., 2012; Schobben et al., 2014;
52	Song et al., 2015) the intense global warming started at the extinction horizon as testified in the
53	Meishan section (South China), and then continued in the Early Triassic, very likely with the
54	release of methane from deep ocean sediments and coals that triggered the process, and the
55	release of additional greenhouse gasses by interactions of the Siberian traps with local
66	permafrost soils, limestones, and other deposits rich in organic matter (e.g. Racki, 2003; Racki &
57	Wignall, 2005; Retallack & Jahren, 2008; Grasby et al., 2011).



68	The hyperthermal had severe effects also on the paleobiogeographic patterns. In the last years
69	the distribution of land tetrapods across the PTME was discussed by a number of studies which
70	however suggested different scenarios. By compiling literature evidence on the main skeletal
71	findings, Sun et al. (2012) suggested that, in the Early Triassic, terrestrial vertebrates totally
72	vacated the equatorial belt, the so-called 'vertebrate equatorial-gap', as a consequence of the
73	extreme hot temperatures. More recently, Bernardi et al. (2015, 2018) reviewed the Late
74	Permian-Early Triassic terrestrial tetrapod record integrating skeletal and track data and
75	concluded that tetrapod geographic distribution was much wider than previously suggested. In
76	the Early Triassic it included also the low latitudes, though polarward dispersals were detected in
77	the Early Triassic and possibly linked to the development of super-hot temperatures in the
78	equatorial belt (Bernardi et al., 2018). Fossil track evidence, in particular, was key in denying the
79	existence of an 'equatorial gap' (Bernardi et al., 2018).
80	Archosaur tracks and trackways are in fact well-known from Lower to Middle Triassic
81	siliciclastic and carbonate sediments of the Upper Buntsandstein and Lower Muschelkalk (late
82	Olenekian-early Anisian) of Germany (Haubold, 1971a, 1971b; Klein & Haubold, 2007), the
83	Lower Triassic of the Holy Cross Mountains in Poland (Klein & Niedzwiedski, 2012), the
84	Middle Triassic of Bourgogne (Gand, 1979), Massif Central (Demathieu, 1970) and Ardèche in
85	France (Courel & Demathieu, 1976), the Iberian Range in Spain (Fortuny et al., 2011; Diaz-
86	Martinez, et al., 2015) and Sardinia in Italy (Citton et al., 2020). Further sites, often with
87	identical ichnotaxa and ichnoassemblages, are known from the Lower to Middle Triassic of
88	Great Britain (King et al., 2005), North American southwest (Klein & Lucas, 2010), Argentina
89	(Melchor & De Valais, 2006), Africa (Klein et al., 2011) and southern China (Xing et al., 2013).
90	In the Alps, chirotherian footprints were described from the Lower to Middle Triassic of the



91	Dolomites, Piedmont and Ligurian Alps in Italy (Avanzini & Mietto, 2008; Petti et al., 2013;
92	Santi et al., 2015), Aar Massif in eastern Switzerland (Feldmann et al., 2009; Klein et al., 2016)
93	and the Aiguilles Rouges Massif (Western Alps), on the border between Switzerland and France
94	(Demathieu & Weidmann, 1982; Avanzini & Cavin, 2009; Cavin et al., 2012; Klein et al., 2016)
95	We here describe and interpret a new archosaur track assemblage from the Gardetta Plateau
96	(Western Alps, south-western Piedmont, Italy; Fig. 1) that was analyzed in two different field
97	works, during the summer 2009 and in the autumn 2017-2018.
98	Tracks are preserved on two distinct track surfaces, belonging to the same stratigraphic
99	horizon. Some of them are badly preserved but distinct trackways, up to 3 m long, can be
100	recognized together with other exceptionally preserved isolated tracks showing clear
101	morphological details of the trackmaker's autopodium.
102	This discovery provides reliable evidence of the presence of archosauriforms in the
103	Briançonnais domain during the Early Triassic, adding further support to the occurrence of
104	terrestrial tetrapods at low latitudes soon after the PTME (Bernardi et al., 2015; 2018) and well-
105	before a full land ecosystem recovery.
106	
107	
108	MATERIALS AND METHODS
109	
110	All the specimens were identified in the same outcrop, located about 1 km SE of the Gardetta
111	Plateau, close to Pianezza creek (44°24'5.75"N; 7° 1'45.29"E; Canosio Municipality, Cuneo
112	Province, NW Italy; Fig. 1).



Most of the footprints are preserved as negative epichnia (concave epirelief) and were left in
situ in the field. The footprints were discovered by EC and MP in summer 2008. A surface of
about 10-15 m <sup>2</sup> was mapped a first time in 2009 by HF and then in 2017 by FP and HF. An
exceptionally preserved trackway, consisting of three large pes and manus imprints, was then
discovered during the 2017 and 2018 field works by EM and FP, about 10 m higher up on the
same outcropping horizon. Tracks outlines were drawn on transparency acetate film and then
digitized by a vector-based drawing software (Adobe Illustrator ©). Additional footprints were
collected by the authors and hikers from loose sandstone slabs in the creek below the track
surfaces. These isolated and usually fragmentary footprints are preserved both as concave
epirelief and well-preserved convex epirelief, the latter being preserved in the basalmost level of
the sandstone bed which overlies the track layer.
Close-range photogrammetry was used to document tracks and obtain three-dimensional
model of the best-preserved ones (Petti et al., 2008; Remondino et al., 2010; Mallison & Wings,
2014). The data processing phase was performed using Agisoft PhotoScan ® Professional
software, following the procedure indicated by Mallison & Wings (2014). In a second phase, the
software Surfer®14 (GoldenSoftware, 2002), was used to convert elevation points to contour
lines and to produce color coded maps of the studied material.
The obtained images are ideal for both precisely measure standard ichological parameters
(Haubold, 1971b; Leonardi, 1987) and for recognizing anatomy related morphologies, therefore
for the reconstruction of the trackmaker's autopodial osteology.
Trackmaker identification was carried out employing three different and integrated
methodological approaches: i) Synapomorphy-based correlation (Olsen, 1995; Carrano &
Wilson, 2001); ii) Phenetic correlation (Carrano & Wilson, 2001) and iii) Coincidence



correlation (Carrano & Wilson, 2001). The synapomorphy-based method focuses on the identification of osteologic-derived character states in the footprints that result from the impression of synapomorphic characters in the trackmaker autopodia (see Olsen et al., 1998; Carrano & Wilson, 2001; Wilson, 2005; Romano et al., 2015). The phenetic correlation is closely linked to ichnotaxonomy and derives from an accurate description of the footprint and the identification of the trackmaker through the recognition of an affinity between tracks and limbs osteology (Carrano & Wilson, 2001; Wilson, 2005). The coincidence correlation is usually adopted to refine trackmaker identification and is based on supplemental data including geological age, geographic provenance, local faunal composition and distributions, and abundances of skeletal taxa and ichnotaxa (Carrano & Wilson, 2001).

## **GEOLOGICAL FRAMEWORK**

The Gardetta Plateau - Preit valley area is located in the southern part of the Western Alps (Fig. 1). It encompasses the Sautron, Rouchouze, Rocca Peroni tectonic units and the Gardetta deformation unit (*sensu* d'Atri et al., 2016) also known as "bande siliceuse de la Gardetta" (Gidon, 1972). These tectonic units pertain to the Briançonnais Domain (Gidon, 1958a, 1958b, 1972; Schmid et al., 2004, 2017) and in particular to the External Briançonnais Domain which is characterized by very low grade to anchizone metamorphism (d'Atri et al., 2016).

The upper Permian-Mesozoic sedimentary succession varies considerably within the Briançonnais Domain *s.l.* (Briançonnais Domain *s.s.* and Ligurian Briançonnais, Decarlis & Lualdi, 2009; Fig. 2) due to the slightly different paleogeographic positions of these sectors (see



160

161

162

163

164

165

166

167

168

169

170

171

172

173

174

175

176

177

178

179

180

181

Decarlis et al., 2013 for a review). The outcropping lithostratigraphic units, even if can be correlated across the distinct domains, display different thickness, vertical/lateral relationships and hiatuses. These differences led authors to adopt a multitude of official and unofficial names for the lithostratigraphic units. Despite these minor differences, the late Permian–Early Triassic sedimentation in the whole Brianconnais domain s.l. testifies to the evolution of a continental margin affected by extensional tectonics. The Brianconnais domain was positioned north of the westernmost sector of the Palaeotethys, in the western continental termination of the Meliata oceanic back-arc basin (Ziegler & Stampfli, 2001; Decarlis et al., 2013). Adopting the paleolatitude calculator developed by Van Hinsbergen et al. (2015) (model version 2.1) and using the Global Apparent Polar Wander Path of Torsvik et al. (2012) as paleomagnetic reference frame, the Early Triassic (250 Ma) palaeolatitude estimate for the Southern Briançonnais Domain is 11.8 N. In the study area the volcano-sedimentary succession starts with upper Carboniferous -Permian volcanic rocks (andesitic lavas followed by rhyolites and rhyolitic ignimbrites) unconformably overlain by upper Permian-Lower Triassic siliciclastic continental-to-transitional deposits (the so called "semelle silicieuse" of French Authors). In particular these deposits are characterized by basal coarse grained conglomerates and quartz-conglomerates, named locally "Verrucano Brianzonese", (Carraro et al., 1970; Cassinis et al., 2018) that evolve upward into quartz-arenites and quartz-siltites of the "Werfenian quartzites" (Fig. 2; Gidon, 1958b; Malaroda, 1970; Megard-Galli & Baud, 1977; Costamagna et al., 2002; Costamagna, 2013). The siliciclastic sequence indicate deposition in an alluvial environment characterized by sandy braided fluvial system fed by the residual Variscan relieves (Costamagna, 2013). In the southernmost part of the Briançonnais domain (External Ligurian Briançonnais Domain,



182	Vanossi, 1974; 1991; Bertok et al., 2012) these latter lithostratigraphic units are known as	
183	"Scytian quartzites" or "Ponte di Nava Quarzites" (Fig. 2; Decarlis et al., 2013, 2015). Similar to	
184	the siliciclastic sequence of the Briançonnais Domain s.s., the "Ponte di Nava Quarzites"	
185	originated from the dismantling and reworking of the Paleozoic igneous and metamorphic	
186	basement.	
187	The quartz-arenites can be topped either by greenish pelites (known as "Case Valmarenca	
188	Pelites" in the Ligurian Briançonnais, Vanossi 1974; 1991), that have been interpreted as mudflat	
189	deposits, or by a thin and discontinuous interval of cavernous dolostones called "Cargneules	
190	Inférieures" representing the sedimentation in an arid environment as an evaporitic sabkha (Fig.	
191	2). According to Lualdi & Seno (1984), in the Ligurian Briançonnais Zone the "Case	
192	Valmarenca Pelites" could be laterally equivalent to the "Cargneules inférieures".	
193	The continental succession and/or the evaporitic deposits are followed by Middle Triassic	
194	shallow water carbonates of the "couverture carbonatée" (Gidon, 1958b; Megard-Galli & Baud,	
195	1977; Costamagna et al., 2002) comprising a lower calcareous complex (Costa Losera Fm,	
196	Lualdi and Bianchi, 1990, corresponding to the e St. Triphon Formation of the classic	
197	Briançonnais Domain) and an upper dolomitic complex (San Pietro dei Monti Fm, Vanossi,	
198	1969). These carbonate deposits testify the sedimentation in a subsiding carbonate ramp.	
199	The lower calcareous complex (Fig. 2) begins with a characteristic facies named "Marbres	
200	Phylliteux" by French Authors made of greyish and brownish fine-grained limestones, (lower to	
201	upper Anisian) with sericite, muscovite, chlorite laminated levels. Bedding can be locally	
202	masked by pervasive and intense bioturbation ("Calcaires Vermiculés" facies) assigned to the	
203	ichnogenus Rhizocorallium. The basal complex ends with varicolored pelites, interpreted as	



cinerites (upper Anisian in age) by Caby & Galli (1964), recognizable throughout the whole Briançonnais Domain.

The upper dolomitic complex (Fig. 2) is constituted by massive to well-bedded dolostones followed by cyclically arranged carbonates ("Calcaires rubanés" – upper Anisian – upper Ladinian; Gidon, 1958b; Megard-Galli & Baud, 1977; Costamagna et al., 2002; Decarlis & Lualdi, 2009) characterized by subtidal crinoidal wackestones, intertidal oolitic limestones and supratidal dolomitic mudstones capped by reddish paleosols, that testify shallowing-upward cycles. The dolomitic succession includes dark limestones, dark fossiliferous and/or oolithic dolostones, meter-thick autoclastic breccias and gypsum–anhydrite pseudomorphs witnesses of major emersion events. These lithofacies, dated to the uppermost Ladinian, are known in the different Briançonnais domains as "Dolomies blanches" or "Dolomies grises" or "Couches a C. goldfussi" or "Complexe schisto-dolomitique basal".

### THE PIANEZZA STRATIGRAPHIC SUCCESSION

In the framework of the abovementioned stratigraphic setting the footprint-bearing level is located in the Pianezza area along the track connecting Colle del Preit (2100 m a.s.l.) to Grange Isoardi (Pianezza area, 2275 m a.s.l.) (Fig. 2). The outcrop is located along the SW flank of a narrow antiformal anticline belonging to the Sautron Tectonic Unit which overthrusts the Rouchouze Tectonic Unit. Here the volcano-stratigraphic succession begins by meta-andesites and andesitic schists pertaining to the upper Carboniferous-Permian volcanic complex. The sedimentary succession continues upward with a thin and discontinuous (up to 1 meter) level of



graphitic schists, deriving from the weathering of the volcanic basement (Lorenzoni & Zanettin, 1958) and is then followed by up to 100 meters of quartz-conglomerates ("Verrucano Brianzonese") and by fine to very fine quartz-arenite and quartz-siltite with ripple marks and cross bedding ("Werfenian quartzites"). The track-bearing horizon occurs at the top of the latter clastic interval. The succession continues upward with 15 meters of gypsum/anhydrite deposits of the lower cargneule. In the Pianezza area the Middle Triassic "couverture carbonatée" is only represented in the north-eastern flank of Sautron Unit anticline.

# CHRONOSTRATIGRAPHIC FRAMEWORK OF THE STUDY AREA

The sedimentary rocks belonging to the quartz-rich clastic succession does not allow precise dating because of the lack of biostratigraphic markers as commonly happen for these kind of deposits. They are here referred to the upper Permian-Lower Triassic on the base of their stratigraphic position in the Sautron Unit, similar to that of the well-comparable quartz-conglomerate and quartzarenite rocks occurring not only in the Briançonnais Domain, but also in the Southern Alps, Sardinia and Provence. For this reason, in order to constrain the age of the track-bearing horizon, some considerations are required: i) the coarse quartz-conglomerates ("Verrucano Brianzonese") are commonly referred to the late Permian-earliest Triassic (Gidon, 1958b; Carraro et al., 1970; Megard-Galli & Baud, 1977; Decarlis & Lualdi, 2009); ii) the Lower Triassic age can be hypothesized considering the occurrence of *Estheria minuta* Alberti and *Myacites fassaensis* Bittner within the "Ponte di Nava Quarzites" (Decarlis & Lualdi, 2009); iii) the "lower cargneule" unit and its lateral equivalent "Case Val Marenca Pelites" are generally



attributed to the late Early Triassic (Gidon, 1958b; Carraro et al., 1970; Megard-Galli & Baud, 1977; Decarlis & Lualdi, 2009); iv) the lower part of "Marbres Phylliteux" are considered early Anisian in age, on the basis of the occurrence of Rhizocorallium, that is regarded to be an early Anisian marker all over the Tethyan realm (Baud, 1976); v) an early Anisian age for the base of the lower calcareous complex ("Marbres Phylliteux" and Costa Losera Fm.) is also suggested by the occurrence of Dasycladacean algae and crinoidal remains (Dadocrinus sp.; Carraro et al., 1970); vi) In the northern Briançonnais of southwestern Switzerland a find of the ammonoid Beyrichites cadoricus in the upper part of the St-Triphon Formation indicate a middle Anisian age (Baud et al., 2016).

Additionally, it is worth mentioning that both in the Geological Map of the Argentera Massif (Malaroda, 1970; Carraro et al., 1970) and in the Geological Map of France at the scale 1: 50.000 (Sheet 896, Larche; Gidon, 1978) the studied outcrop was attributed to Lower Triassic. All the above reported data thus point to a probable attribution of the trampled horizon to the late Early Triassic.

### SYSTEMATIC ICHNOLOGY

Most footprints are preserved as natural molds (concave epirelief) on top of a 3-4 cm thick bed of fine sandstone. The tracks are shallow, less than 2 cm deep, but most of them are cut by small-scale tectonic cracks/fissures and strongly weathered. Two possible trackways with lengths of 4–5 m were identified on a track surface. Only one isolated track was visible on the underlying sandstone bed, also preserved as concave epirelief. Three solitary small footprints,





273	preserved as convex epirelief of the directly overlying sandstone bed, were collected from loose
274	slabs. The upper surface of this 1–2 cm thick sandstone bed is marked by symmetric wave
275	ripples, exposed on a spectacular bedding plane (Fig. 3).
276	An exceptionally preserved trackway, made of three consecutive manus-pes sets was found on
277	another surface, belonging to the same stratigraphic horizon, upstream of the previously
278	described ones (Fig. 4). The general features of the herein studied ichnoassemblage are typical
279	for chirotherian tracks (Haubold & Klein, 2002).
280	
281	
282	Ichnogenus Chirotherium Kaup, 1835
283	Type ichnospecies: Chirotherium barthii Kaup, 1835
284	
285	Chirotherium isp.
286	(Figs 3, 7)
287	<b>Referred specimens:</b> two trackways preserved as concave epirelief (GT-1 and GT-2). GT-1
288	consists of four clear and two weakly impressed imprints, arranged in a 2.10 m-long trackway in
289	the lower part of the outcrop, just 2 meters above the creek level (Fig. 3). Its direction on the
290	steep bedding plane points upwards to southeast. Trackway GT-2 is 2.40-m-long, is preserved in
291	the lower part of the same bedding plane, about 2 meters above the creek level, running from
292	northwest to southeast.
293	
294	Description: pentadactyl and semi-digitigrade pes imprint. Pes is longer than wide, (Foot
295	Length [FL] = 13 to 16 cm; Foot Width [FW] = $8-10$ cm; FL/FW = $1.6$ to $2.0$ ) with digit group



II-IV roughly asymmetrical. Pedal digit impressions gradually increase from I to IV, with II subequal or shorter than digit IV; digit III is the longest. In the best-preserved track (GT1-3; Figs 3, 7), digit I is pointed and placed posteriorly with respect to digit group II-IV. Digit V is oval and tapers distally; it is positioned posteriorly and laterally to digit I-IV and directed antero-laterally. No digital pad impressions can be observed on digit II-IV. Digit V shows a large rounded pad impression and a possible sub-triangular shaped claw mark. Manus tracks are absent or faintly preserved as small semi-circular imprints, placed in front of the pedal footprints. An isolated tetradactyl imprints, measuring 4.5 cm in length and 7 cm in width, and another isolated circular pentadactyl imprint 5.5 cm long are interpreted as possible manus imprints.

In the trackway the oblique pace varies between 26 and 41 cm, with a mean value of 36 cm. The pes pace angulation varies between 145° and 165°, with a mean value of 157°.

**Discussion:** the ichnogenus *Chirotherium* with its holotype *Chirotherium barthii*, was described by Kaup (1835) on trackways from the "Thüringischer Chirotheriensandstein" (Lower-Middle Triassic) of the Thuringia region (Germany). The here described material, even if not perfectly preserved, retains some diagnostic features of the ichnogenus *Chirotherium*, such as the oval morphology and the position of digit V (slightly behind digit group II-IV), and the relative digit length of group II-IV, with digit IV longer or sub-equal to digit II. Pes pace angulation is also similar to the values to date reported for the ichnogenus (160°-170°). *Chirotherium barthii* (Figs 7e, 7f) shows clear circular pads on digit group II-IV and digit impressions are broader than in the studied specimens. In *C. barthii*, as well as in *C. rex*, *C. moquinense* and *C. vorbachi* (Fig. 7h), digits I-IV are splayed whereas in the GT-1 and GT-2 trackways, pedal digits outlines are closely arranged with only digit I medially spread. Digits II-IV seems to be almost parallel to





319	each other and the digit pattern resemble that of the ichnospecies C. sickleri Kaup, 1835 (Figs 7i,
320	71, 7m) with digit I forming a narrow group with digits II, III and IV. Nevertheless, digit IV,
321	though slightly shorter than III, is not much longer than II as observed in most of the specimens
322	assigned to C. sickleri. Unfortunately, the bad preservation of pes imprints in GT-1 and GT-2
323	trackways preclude any accurate ichnospecific assignment.
324	
325	Ichnogenus Isochirotherium Haubold, 1971a (Figs 4, 5, 8)
326	Type ichnospescies: Isochirotherium soergeli (Haubold, 1967).
327	
328	Isochirotherium gardettae ichnosp. nov.
329	
330	<b>Derivatio nominis:</b> from the Gardetta plateau, type locality of the ichnospecies.
331	
332	Type-level: "Werfenian quartzites", Lower Triassic.
333	
334	Referred specimens: a trackway made of three well-preserved and consecutive manus-pes
335	couples (GT-7; Fig. 4) not exceeding 2.20 m across. Another possible isolated track (GT-3)
336	partially preserved in the lower track surface.
337	
338	Diagnosis: chirotherian track with pentadactyl pes and small and tetradactyl manus imprint
339	and pes digit IV noticeably shorter than II; pes digit group I-IV slightly longer than wide, pes
340	digit V with large ovoid metatarsal pad and a reduced phalangeal portion. Pes length ranging





from 28 to 33 cm; cross axis equal to 90°. Trackway very narrow, pace angulation near 165°, and ratio of stride to pes length is 4.3.

343

344

345

346

347

348

349

350

351

352

353

354

355

356

357

358

359

360

361

362

363

**Description:** pentadactyl and semi-plantigrade pes imprint, longer than wide (FL = 33.4 cm; FW = 19.2 cm; FL/FW = 1.74). Digit III is the longest. It is slightly longer than II, whereas digit IV is shorter than II. Digit I is the shortest and is thinner than those of digit group II-IV. The total divarication I-IV is 22°; the angle between digit I and II is 8° and is equal to that between II and III but larger than II-IV (6°). Cross axis is nearly equal to 90°. Digit impressions are robust and pointed showing large sub-triangular claw marks. Two phalangeal pad impressions are present on each digit of group I-IV. The metatarsal-phalangeal portion is proximally arched and could be separated from digit V by a gap, or joined with it through a convex area, running from the basalmost portion of digit I to the medial digit V. Digit V shows a large oval impression joined to a rounded phalangeal-ungual portion, laterally spread out. In GT-7-2 and GT-7-3, pes digit V has a sub-triangular shape with a wider inner margin, almost aligned with the medial margin of digit I. Length of pes digits are: I) 118 mm; II) 173 mm; III) 186 mm; IV) 136 mm; V) 167 mm. The manus is small, tetradactyl and digitigrade, wider than long (FL = 8.04 cm; FW = 13 cm; FL/FW = 0.62) and is placed in front of the pes. Digits are short and pointed. Digits II and III have nearly equal length and are longer than digits I and IV; the latter is moderately spread outward. Digit IV is possibly the shortest. Length of manus digits are: I) 49 mm; II) 74 mm; III) 68 mm; IV) 43 mm. The trackway, made by three consecutive manus-pes sets, shows a clear narrow gait (pace angulation 164°). Oblique pace is 59 cm, whereas double pace is 119 cm across. Manus-pes couples turned slightly outward with respect to the midline (from 10° to 15° on average).

1	$\sim 1$	
≺	hД	

<b>Discussion:</b> the ichnogenus <i>Isochirotherium</i> was erected by Haubold (1971a); its type
ichnospecies I. soergeli (Haubold, 1967) comes, as for Chirotherium barthii, from the
"Thüringischer Chirotheriensandstein" (Lower-Middle Triassic) of the Thuringia region
(Germany). The ichnogenus is reported also from the Middle Triassic of Great Britain (Tresise &
Sarjeant, 1997; King et al., 2005), from the Lower-Middle Triassic of North American
Southwest (Peabody, 1948; Klein & Lucas, 2010), the Aiguilles Rouges Massif (Western Alps)
on the border between Switzerland and France (Avanzini & Cavin, 2009; Klein et al., 2016) and
from the Middle Triassic of North-East Italy (Avanzini & Leonardi, 2002).
The main diagnostic features of this ichnogenus, retained by our specimens are: i) the relative
digit length, with digit II longer than IV and shorter than III; ii) a marked heteropody; iii) the pes
pace angulation around 165°; iv) the weakly impressed distal portion of digit V and v) pes-
manus couples outward rotation of about 15°. However, the studied trackway shows clear
difference to most of the ichnospecies known to date. For example, the type ichnospecies $I$ .
soergeli Haubold, 1967 (Fig. 8o), has smaller absolute dimensions, thinner pes digit marks and,
most importantly, display five clear digit impressions in the manus contrary to GT-7, where only
tetradactyl manus were observed.
Isochirotherium hessbergense Haubold, 1971a (Fig. 8m) has also a pentadactyl manus and is
clearly different from the material described in this paper for its digit group I-IV longer than
wider and for the relative pes digit length, notably digit I is longer than IV.
Isochirotherium demathieui Haubold, 1971a (Fig. 8n) can be excluded for its pentadactyl
manus and for the shorter distance between manus and pes.



386	Isochirotherium coltoni Peabody, 1948 (Fig. 8h) and I. lomasi Baird, 1954 (Fig. 8i) retain
387	much slenderer digit impressions, especially in the pes imprint and most notably have manus
388	tracks more internally placed than in the studied footprints. Interestingly I. herculis Egerton,
389	1839 (Fig. 8e) has similar dimensions (i.e. FL longer than 30 cm) but can also be excluded for i)
390	the tridactyl manus; ii) the digit group I-IV slightly wider than longer and iii) the manus imprint
391	position, very close to that of the pes.
392	Isochirotherium marshalli Peabody, 1948 (Fig. 8f) shows similar features such as: i) the pes
393	digit relative length; ii) the interdigital angles values; iii) the digit group I-IV as longer as wider;
394	iv) the arched metatarsal-phalangeal portion; v) the configuration of digit V whose phalangeal
395	portion is significantly smaller than the ovoidal and possibly tarsal-metatarsal pad. Nevertheless,
396	the assignment to this ichnospecies is precluded by its pentadactyl manus.
397	Isochirotherium inferni Avanzini & Leonardi, 2002 from the Illyrian (late Anisian, Middle
398	Triassic; Fig. 8g) of the Adige Valley (Bolzano, NE Italy) closely resembles the Gardetta
399	specimens for: i) the arched metatarsal-phalangeal portion; ii) the position of the base of pes digit
400	V, placed along the axis of digit III; iii) pes digit relative length; iv) cross axis equal to 90° v) pes
401	angulation of about 160°; vi) positive rotation of manus-pes couples respect to the midline (10°-
402	15°). However, pes digits are stouter and the manus is described as pentadactyl (even if in the
403	outline drawing only four digits are clearly appreciable). The tracks referred to Isochirotherium
404	delicatum Courel & Demathieu, 1976 and found in the Anisian-Ladinian deposits of Argentière
405	(Ardèche, France; Courel & Demathieu, 1976; Courel et al., 1979; Demathieu, 1984; Gand,
406	1978) and Gampempass (Southern Alps, Italy; Avanzini & Lockley, 2002) show less-thick digit
407	impressions and a markedly reduced digits IV and V; the latter is also much more backward
408	positioned if compared with the studied specimens.



We therefore erect the new ichnospecies *Isochirotherium gardettae* to describe a new and well-preserved *Isochirotherium* trackway that differs from all the other ichnospecies for all the features listed above.

412

409

410

411

### TRACKMAKER IDENTIFICATION

414

415

416

417

418

419

420

421

422

423

424

425

426

427

428

429

430

413

Grounding on previous studies and new observations Bernardi et al. (2015) showed that chirotherian footprints, such as Protochirotherium, Chirotherium, Brachychirotherium and *Isochirotherium*, can be confidently attributed to archosauriforms, based on the presence of a digit IV shorter or as long as digit III. Being metatarsal length directly proportionate to digit length, this assumes that metatarsal IV is shorter than or as long as metatarsal III, a synapomorphy of the archosauriforms (Nesbitt, 2011). Other characters useful to identify archosauriforms traces are: i) the presence of a compact digit group I-IV; ii) a posterolateral positioned and strongly reduced digit V; iii) a massive metatarsal-phalangeal region, shorter than or as long as digit I. However, the first character occurs in archosauriforms and non archosauromorphs diapsids (Haubold, 1971a, 1971b; Smith & Evans, 1996) whereas the second is present in archosauriforms, lepidosaurs and basal archosauromorphs (Haubold, 1971a, 1971b; Evans & Wang, 2005; Gottman-Quesada & Sander, 2009). Other features suggesting an archosaur affinity for chirotherian footprints (observed also in the here described traces), are narrow trackways linked to the disposition of limbs under the body, and the presence of small manus relative to the pes, which indicate a possible early tendency toward bipedal posture and gate (see Haubold, 1971a, 1971b, 1984, 2006; Klein et al., 2010).



431	To reconstruct the hind- and fore-limb autopodial bones, we assumed an arthral position for
432	the joint articulations within digital pad impressions (Fig. 9a).
433	In our opinion, the sub-elliptical to pyriform impression behind group I-IV in <i>Isochirotherium</i>
434	could be the result of the coalescence of the impression of the phalangeal-metatarsal portion of
435	digit V and of a thick fleshy pad beneath the astragalus, the calcaneus and some of the tarsal
436	bones. Overall, the trackmaker's pes may have had a semi-plantigrade posture, as evidenced by
437	the gap between digit group I-IV and digit V, corresponding to the part of the foot held up during
438	locomotion. The manus has a marked digitigrade posture and its tetradactyly might result by the
439	fact that manual digit V likely held off the ground during the touch-down and weight bearing
440	phases (sensu Manning, 2004).
441	The reconstructions thus obtained shows the following pes and manus phalangeal formulas:
442	pes 2-3-4-4-1 and manus 1-2-3-3. They are compared with the anterior and posterior limbs of the
443	main groups of archosauriforms known in the Triassic period (Huene, 1902; Broom, 1903; 1905;
444	Romer, 1971; Welles, 1947; Young, 1964; Zhang, 1975; Peyer et al., 2008; Ezcurra et al., 2013;
445	Sookias & Butler, 2013; Trotteyn et al., 2013).
446	The first considered non-archosaurian archosauriforms groups are Proterosuchidae (Ezcurra et
447	al., 2013), Proterochampsidae (Trotteyn et al., 2013) and Euparkeriidae (Sookias & Butler,
448	2013). In all the three representatives <i>Proterosuchus fergusi</i> Broom, 1903 (South Africa,
449	Induan-?early Olenekian; Fig. 9e), Chanaresuchus bonapartei Romer, 1971 (Argentina,
450	Ladinian; Fig. 9i) and Euparkeria capensis Broom, 1913 (South Africa, Anisian; Fig. 9h), the IV
451	metarsal has a length similar or greater than that of the III but the digit II is much shorter than
452	digit III and nearly equal to digit IV, in contrast to what we observe in specimens GT-7-1, GT-7-



453	2 and GT-3. No fore- or hind limb bones are known for the Doswelliidae, another clade of non-
454	archosaurian archosauriforms (Middle-Late Triassic; Sues et al., 2013).
455	Diedrich (2015) recently attributed the Isochirotherium tracks to Arizonasaurus Welles, 1947
456	a member of Poposauroidea (archosaurian archosauriforms) found in the Moenkopi Formation
457	(Arizona, USA, Anisian,), from the same levels as Isochirotherium tracks. Unfortunately, no
458	bones of the fore- and hind-limbs are known from Arizonasaurus, as well as from
459	Ctenosauriscus koeneni (Huene, 1902) (Germany, latest Olenekian), the Lower Triassic
460	poposauroid arehosaur, and additionally findings are needed to test Diedrich's hypothesis.
461	The hind-limb bones are known in <i>Lotosaurus adentus</i> Zhang, 1975 (China, Ladinian; Fig.
462	9d), another member of Poposauroidea with semi-plantigrade posture. If compared with the
463	restored autopodium, it is characterized by larger fore-limbs, V digit positioned further forward,
464	longer metatarsals of digit group I-IV and different digit proportions.
465	The pedal phalangeal relative length of the rauisuchid archosaur Postosuchus alisonae Peyer
466	et al., 2008 (USA, Norian; Fig. 9c), is similar but all the five metatarsals are much longer,
467	implying a digitigrade posture, as in the reconstruction proposed by Peyer et al. (2008).
468	Postosuchus kirkpatricki Chatterjee, 1985 (USA, Norian; Fig. 9b), is also characterized by
469	very long metatarsals and thus excluded as a possible trackmaker. The smaller but complete
470	skeleton of <i>Ticinosuchus ferox</i> Krebs, 1965 (see Lautenschlager & Desojo, 2011 for a review of
471	the species) from the uppermost Anisian of Monte San Giorgio (southern Switzerland), shows
472	long metatarsals and a digit IV longer than digit II and is commonly considered as the producer
473	of Chirotherium trackway (Haubold, 1984, 1986).
474	By contrast, the hind limbs of the non-archosaurian archosauriform clade of Erythrosuchidae
475	(Ezcurra et al., 2013) are characterized by relative digit length very similar to that outlined for



497

498

Isochirotherium gardettae and a pedal phalangeal formula that is approximately 2-3-4-5-3 (Young, 1964; Cruickshank, 1978; Gower, 1996). 477 Metatarsals II and III are sub-equal and slightly longer than IV in Erythrosuchus africanus 478 Broom, 1905 (South Africa, lower Anisian; Fig. 9f. See also Cruickshank, 1978; Gower, 1996). 479 Metatarsals II and III are the longest in *Shansisuchus shansisuchus* Young, 1964 (Fig. 9g), 480 481 another member of Erythrosuchidae found in upper Anisian deposits of China; S. shansisuchus also possesses a hook-shaped proximal end of metatarsal V and its relative digit proportion 482 closely fits that of our individual, but as for E. africanus digit V seems to be too forwardly 483 positioned. However, digit V impression in *I. gardettae* likely records only the distal metatarsal 484 and phalangeal (ungual) portions. During locomotion the former was held off the ground 485 whereas the latter was likely being retracted due to the presence of a thick fleshy pad beneath 486 calcaneum and astragalus. 487 The morphology of the acetabulum and proximal end of the femur in erythrosuchids suggests 488 a distinctly sprawling gait (Gower, 2003; Ezcurra et al., 2013), that clashes with the narrow 489 trackway seen in *I. gardettae*. Nevertheless, the prominence of metatarsal II and III is evidenced 490 only in non-archosaurian archosauriforms (Gower, 1996) and thus an individual belonging to this 491 492 group, possibly a yet unknown taxon and with a more erect stance and characterized by a marked heteropody, is the most suitable producer (Fig. 10). 493 494 495 **BIOCHRONOLOGY AND BIOGEOGRAPHY** The Gardetta ichnoassemblage represented by *Chirotherium* and *Isochirotherium* is typical 496

for terrestrial deposits of the late Olenekian and early Anisian (Klein & Haubold, 2007) and the

Gardetta chirotheriid tracks correlate with the international *Chirotherium barthii* Assemblage

Peer| reviewing PDF | (2020:08:51782:0:1:NEW 10 Aug 2020)



499	Zone of Klein & Lucas (2010a). This biochron is characterized by the occurrence of
500	Chirotherium and Isochirotherium, but also by two other ichnogenera not present at Gardetta,
501	Rotodactylus, and Synaptychium. The Chirotherium barthii Assemblage Zone ranges from the
502	late Early to early Middle Triassic (late Olenekian – early Anisian), and independently confirms
503	the Early Triassic (?Olenekian) age, derived by stratigraphic correlation with other sections in
504	the Briançonnais of the Western Alps.
505	The Gardetta outcrop enlarges also the knowledge on biogeography of archosaurs in the
506	Lower Triassic of Europe, so far based on archosaur ichnosites discovered in Italy (Val Marenca,
507	Santi et al., 2015; Sardinia, Citton et al., 2020), Spain (Moncayo and Tagamanent, Díaz-Martínez
508	& Pérez-García, 2012), Switzerland (Cascade d'Emaney and Vieux Emosson; Cavin et al.,
509	2012), Austria (Drau Range; Krainer et al., 2012), Germany (Bundsandstein; Klein & Haubold,
510	2007) and Poland (Wióry, Holy Cross Mountains, Klein & Niedźwiedzki, 2012).
511	Early Triassic erythrosuchid skeletal fossils are known from the late Olenekian of Russia,
512	South Africa, China and India (see Gower, 2003; Ezcurra et al., 2013, 2019, 2020; Gower et al.,
513	2014; Ezcurra, 2016). The Gardetta ichnosite testifies the presence of erythrosuchids and more
514	generally of Archosauriformes at low latitudes (11.8° N) also during the Early Triassic (Fig. 11).
515	This supports the conclusions of Bernardi et al. (2015, 2018) that Early Triassic ichnosites are
516	mainly distributed along the tropics, contrasting the pattern described by skeletal findings and the
517	hypothesis of a low-latitude vacancy of continental tetrapods during or soon after the PTME
518	(Sun et al., 2012).

520

# **Discussion and conclusions**



The Gardetta ichnosite is characterized by archosaur footprints assigned to <i>Chirotherium</i> isp.
and to the new ichnospecies Isochirotherium gardettae ichnosp. nov. They represent the first
record of terrestrial tetrapods in the Briançonnais domain of the Western Alps and expand the
record of archosaur footprints in the Lower Triassic of Central Europe.
The morphological characters of the tracks assigned to <i>Isochirotherium gardettae</i> ichnosp.
nov. suggest a non-archosaurian archosauriform (Erythrosuchidae?) as possible trackmaker
candidate (even though the presence of crown-archosaurs cannot be excluded), thus providing
crucial information about continental tetrapod occurrence in Europe in the Early Triassic. Based
on a phylogenetic dataset made by 108 middle Permian-early Late Triassic species, Ezcurra &
Butler (2015) investigate principal patterns of early archosauromorph biodiversity change across
the Permo-Triassic mass extinction. The study, performed using phylogenetic diversity,
morphological disparity, number of species and rates of phenotypic evolution across 35 million
years of early archosauromorph evolution, indicates consistent phylogenetic diversification of
the clade in the Olenekian. In particular, the basal diversification of main taxa, which include
erythrosuchids, rhynchosaurs and tanystropheids, resulted in significantly high evolutionary
rates, with a diversification interpreted by the authors as a radiative response to vacant ecological
space, made available by the EPME (Ezcurra & Butler, 2015). If the trackmakers' attribution for
the here described footprints is correct, the material from Gardetta could represent an evidence
from Europe of such radiation, with an archosauromorph fauna composed at least by
?erythrosuchids ( <i>Isochirotherium gardettae</i> ) and pseudosuchids ( <i>Chirotherium</i> isp.). Such clades
as putative trackmaker for the Gardetta traces are well-compatible with an Early Triassic (likely
late Early Triassic) age, considering that the early history of Archosauriformes is represented
essentially by members of Proterosuchidae and Erythrosuchidae (Charig & Reig, 1970;



al., 2013). 545 Following the huge Permo-Triassic biotic crisis, unfavorable environmental conditions 546 characterized much of the Early Triassic, testifying one of the slowest recoveries for ecosystems 547 after an extinction in Earth history. A period between five and nine million years for a full 548 549 recovery has been proposed in several contributions (Hallam, 1991; Erwin, 1992, 2001; Payne et al., 2004, 2011; Algeo et al., 2011; Whiteside & Ward, 2011), inferring a fully restored complex 550 ecosystems only at the beginning of the Middle Triassic (see Chen & Benton, 2012). Such long 551 recovery time led to a revolution on both marine and terrestrial ecosystems (Chen & Benton, 552 2012), with a major influence in the evolution of crucial vertebrates clades in the rest of 553 Mesozoic and Cenozoic eras (Sepkoski, 1984; Benton, 2010). The recovery period led to the 554 emergence of totally new groups, with a rapid diversification of several lineages of sauropsid 555 both on sea and land (Nesbitt et al., 2010; Butler et al., 2011; Gower et al., 2014; Scheyer et al., 556 2014; Motani et al., 2015a, 2015b; Peecook et al., 2018). Avemetatarsalians (which include 557 dinosaurs and pterosaurs) originated in this period (Brusatte et al., 2010; Nesbitt et al., 2010; 558 Chen & Benton, 2012; Benton et al., 2014), along with the evolution of crucial modern group 559 560 ancestors, including crocodiles, lizards, turtles, frogs and mammals. All these aspects highlight the crucial importance of the Early Triassic in the ecosystems restructuring after the Permo-561 Triassic mass extinction. 562 563 Retallack et al. (2011) propose that the long recovery from the mass extinction was strongly influenced by repeated greenhouse crises during the Early Triassic, with consistent negative 564 565 excursions in carbon isotope ratios indicating at least five greenhouse crises in the 5 Myr 566 following the EPME (Induan-Anisian) (see Kidder & Worsley, 2004; Retallack, 2005, 2009,

Cruickshank, 1972; Charig & Sues, 1976; Gower & Sennikov, 2000; Gower, 2003; Ezcurra et



568

569

570

571

572

573

574

575

576

577

578

579

580

581

582

583

584

585

586

587

588

2013; Graisby et al., 2011; Retallack et al., 2011; Sun et al., 2012; Chen & Benton, 2012). In this regard, according to Sun et al. (2012) the entire Early Triassic was characterized by temperatures consistently in excess with respect to the modern equatorial annual sea surface temperatures (SSTs), thus exceeding a tolerable threshold for life in both oceans and land. Inferring SSTs approaching 40°C, according to Sun et al. (2012) the temperature on land very likely fluctuated to even higher levels, with terrestrial tetrapods generally absent between 30°N and 40°S in the Early Triassic. In this framework, and although some uncertainties on the chronological attribution persists, the Gardetta ichnosite provides important evidence to the low latitude distribution of archosaurus during the Early Triassic period, soon after the PTME, confirming the pattern described by Bernardi et al. (2018). In particular, the new discovery provides further evidence for an early recovery terrestrial ecosystems and the presence at low latitudes of archosauriformes during the Early Triassic. Such evidences support a model in which the EPME did not completely vacate low-latitude lands from tetrapods that, therefore would, have been able to cope with the extreme hot temperatures of Pangaea mainland. According to Botha and Smith (2006), Archosauromorpha (along with Procolophonomorpha) could be pre-adapted to extremely arid and hot environment conditions, considering that extant reptiles rarely drink water, excrete quite dry fecal pellets, and are characterized by solute-linked water reabsorption mechanisms, water-resistant integument and low ventilation rates (Withers, 1992; Pough et al., 1996). Such physiological aspects and water conserving mechanisms, probably suggest that the archosaurus response to the extreme hot condition of the Early Triassic (Benton, 2018) have probably been much more efficient and plastic than previously thought, and





did not necessarily imply massive dispersal towards higher latitudes as previously suggested 589 (Sun et al., 2012). 590 Different anatomical features described above indicate a possible ?Erythrosuchids as the most 591 probable trackmaker for the new described ichnospecies *Isochirotherium gardettae*. This 592 attribution can also be supported by track parameters such a narrow trackway and high pace 593 594 angulation, which indicate a more upright posture with respect to a classic plesiomorphic sprawling gait (see Kubo & Benton, 2007). In particular, according to Ezcurra et al. (2013), 595 erythrosuchids were heavily built and characterized by a probably less sprawling gait, when 596 compared to the condition observed in proterosuchids. The narrow trackway, along with 597 consistently high pace angulation in the Gardetta material, also confirm the statement by Kubo & 598 Benton (2009) that, even if proterosuchids and erythrosuchids are traditionally considered as 599 sprawlers, ichnological evidences indicate that more derived erect-limbed archosaurian already 600 evolved in the Early Triassic; the latter conclusion is also supported on the base of ghost ranges 601 from cladograms (Sereno, 1991; Benton, 1999), and fragmentary materials from Russia (Gower 602 & Sennikov, <u>200</u>0). 603 To date, Erythrosuchids are totally unknown from North America and Europe, being 604 605 described only from Russia, South Africa, China and India (see Gower, 2003; Ezcurra et al., 2013, 2019, 2020; Gower et al., 2014; Ezcurra, 2016). The material from the Lower Triassic 606 607 deposits of Gardetta thus could represent the first occurrence of the clade in Europe, although, as 608 already pointed out, the attribution is for the moment only tentative, and new studies are underway to better constrain the identity of the zoological trackmaker. 609



611

612

613

614

615

616

617

618

619

620

621

622

623

624

625

626

627

628

629

630

631

The planned future excavations in the Gardetta ichnosite will hopefully provide additional data to improve our knowledge of the evolutionary history of Archosauriformes in the aftermath of the EPME. ELECTRONIC SUPPLEMENTARY MATERIAL This article contains electronic supplementary material. **ACKNOWLEDGMENTS** We warmly thank the Associazione Escarton that generously supported by this research during the field campaigns held in 2009, 2017 and 2018. A special thanks to Giovanni Raggi for his valuable and constant support during the field works and the project organisation. We acknowledge insightful discussions with A. d'Atri (University of Torino). The authors wish also to thank Dr. Debora Rocchietti (Soprintendenza Archeologia Belle Arti e Paesaggio per le province di Alessandria, Asti e Cuneo) and Dr. Attilio Dalmasso (Museo dei fossili in San Rocco di Bernezzo) and Fabio Manucci for video production and artwork. Finally, a special thank is also due to Hanna Luginbühl for her help in mapping 2009 and to Cecilia Gomiero, Jacopo Valori and Nicolò Amoruso for their precious help during 2018 fieldwork. This paper is part of the project 'The end-Permian mass extinction in the Southern and Eastern Alps: extinction rates versus taphonomic biases in different depositional environments' financed by the Euregio Science Fund (call 2014, IPN16) of the Europaregion Euregio. REFERENCES

PeerJ reviewing PDF | (2020:08:51782:0:1:NEW 10 Aug 2020)



- 632 Algeo TJ, Chen ZQ, Fraiser ML, Twitchett RJ. 2011. Terrestrial-marine teleconnections in
- the collapse and rebuilding of Early Triassic marine ecosystems. *Palaeogeography*,
- Palaeoclimatology, Palaeoecology **308(1-2)**:1-11.
- 635 Alroy J. 2003. Global databases will yield reliable measures of global biodiversity. *Paleobiology*
- **29(1)**:26-29.
- 637 Avanzini M, Cavin L. 2009. A new *Isochirotherium* trackway from the Triassic of Vieux
- Emosson, SW Switzerland: stratigraphic implications. Swiss Journal of Geosciences 102:353-
- 639 361.
- 640 Avanzini M, Leonardi G. 2002. Isochirotherium inferni ichnosp. n. in the upper Anisian
- (Illyrian) of Adige Valley (bozen, Italy). Bollettino della Società Paleontologica Italiana
- **41**:41-50.
- 643 Avanzini M, Lockley M. 2002. Middle Triassic archosaur population structure: interpretation
- based on *Isochirotherium delicatum* fossil footprints (Southern Alps, Italy).
- Palaeogeography, Palaeoclimatology, Palaeoecology, **185(3-4)**: 391-402.
- 646 Avanzini M, Mietto P. 2008. Lower and Middle Triassic footprint-based biochronology in the
- Italian Southern Alps. *Oryctos* **8**:3-13.
- **Baird D. 1954**. *Chirotherium lulli*, a pseudosuchian reptile from New Jersey. *Museum of*
- 649 *Comparative Zoology Bulletin* **111**:165-192.
- 650 **Baud A. 1976**. Les terriers de Crustacés décapodes et l'origine de certains facies du Trias
- carbonaté. *Eclogae Geologicae Helvetiae* **69(2)**:415-424.
- Baud A, Plasencia P, Hirsch F, Richoz S. 2016. Revised middle Triassic stratigraphy of the
- Swiss Prealps based on conodonts and correlation to the Brianconnais (Western Alps). Swiss
- 654 *Journal of Geosciences* **109**:365–377.



- **Benton MJ. 1999.** *Scleromochlus taylori* and the origin of dinosaurs and pterosaurs.
- 656 Philosophical Transactions of the Royal Society of London. Series B: Biological Sciences
- **354(1388)**:1423-1446.
- 658 **Benton MJ. 2003**. When life nearly died: the greatest mass extinction of all time. Thames &
- Hudson, London.
- **Benton MJ. 2010**. The origins of modern biodiversity on land. *Philosophical Transactions of the*
- 661 *Royal Society B: Biological Sciences* **365(1558)**:3667-3679.
- 662 Benton MJ. 2018. Hyperthermal-driven mass extinctions: killing models during the Permian-
- Triassic mass extinction. *Philosophical Transactions of the Royal Society A* **376**:20170076.
- **Benton M, Newell AJ. 2014**. Impacts of global warming on Permo-Triassic terrestrial
- ecosystems. *Gondwana Research* **25**:1308–1337.
- **Benton MJ, Twitchett RJ. 2003**. How to kill (almost) all life: the end–Permian extinction event.
- 667 *Trends in Ecology & Evolution* **18**:358–365.
- **Benton MJ, Forth J, Langer MC. 2014**. Models for the rise of the dinosaurs. Current Biology
- **24**:R87–R95.
- 670 **Bernardi M, Petti FM, Benton MJ. 2018**. Tetrapod distribution and temperature rise during the
- Permian- Triassic mass extinction. *Proceedings of the Royal Society of London B*
- **285**:20172331.
- 673 **Bernardi M, Klein H, Petti FM, Ezcurra MD. 2015**. The Origin and Early Radiation of
- Archosauriforms: Integrating the Skeletal and Footprint Record. *PLoSONE* **10(6)**:e0128449.
- 675 **Berner RA. 2002**. Examination of hypotheses for the Permo–Triassic boundary extinction by
- carbon cycle modeling. Proceedings of the National Academy of Sciences, U.S.A. 99:4172–
- 677 4177.



0/8	bertok C, Martire L, Perotti E, u Atri A, Piana F. 2012. Knometre-scale palaeoescarpments
679	as evidence for Cretaceous synsedimentary tectonics in the External Briançonnais Domain
680	(Ligurian Alps, Italy). Sedimentary Geology 251:58-75.
681	Botha J, Smith RMH. 2006. Rapid vertebrate recuperation in the Karoo Basin of South Africa
682	following the end-Permian extinction. <i>Journal of African Earth Sciences</i> <b>45</b> :502–514.
683	Broom R. 1903. On a new reptile (Proterosuchus fergusi) from the Karroo beds of Tarkastad,
684	South Africa. Annals of the South African Museum 4:159-164.
685	Broom R. 1905. Notice of some new reptiles from the Karoo Beds of South Africa. Records of
686	the Albany Museum 1:331-337.
687	Broom R. 1913. Note on Mesosuchus browni, Watson, and on a new South African Triassic
688	pseudosuchian (Euparkeria capensis). Records of the Albany Museum 2: 394-396.
689	Brusatte SL, Benton MJ, Desojo JB, Langer MC. 2010. The higher-level phylogeny of
690	Archosauria (Tetrapoda: Diapsida). Journal of Systematic Palaeontology 8(1):3-47.
691	Butler RJ, Brusatte SL, Reich M, Nesbitt SJ, Schoch RR, Hornung JJ. 2011. The sail-
692	backed reptile Ctenosauriscus from the latest Early Triassic of Germany and the timing and
693	biogeography of the early archosaur radiation. <i>PloS ONE</i> <b>6(10)</b> :e25693.
694	Caby R, Galli J. 1964. Existence de cinérites et tufs volcaniques dans le Trias moyen de la zone
695	briançonnaise. Comptes Rendus de l'Académie des Sciences de Paris 259:417-420.
696	Carrano MT, Wilson JA. 2001. Taxon distributions and the tetrapod track record. Paleobiology
697	<b>27(3)</b> :564-582.
698	Carraro F, Dal Piaz GV, Franceschetti B, Malaroda R, Sturani C, Zanella E. 1970. Carta
699	Geologica del massiccio dell'Argentera alla scala 1: 50.000 e Note Illustrative. Memorie della
700	Società Geologica Italiana 9:557-663.



- 701 Cassinis G, Perotti C, Santi G. 2018. Post-Variscan Verrucano-like deposits in Italy, and the
- onset of the alpine tectono-sedimentary cycle. *Earth-Science Reviews* **185**:476-497.
- 703 Cavin L, Avanzini M, Bernardi M, Piuz A, Proz PA, Meister C, Boissonnas J, Meyer CA.
- 704 **2012**. New vertebrate trackways from the autochthonous cover of the Aiguilles Rouges
- Massif and reevaluation of the dinosaur record in the Valais, SW Switzerland. Swiss Journal
- 706 *of Palaeontology* **131**:317-324.
- 707 Charig AJ, Reig OA. 1970. The classification of the Proterosuchia. Biological Journal of the
- 708 *Linnean Society* **2(2)**:125-171.
- 709 Charig AJ, Sues H-D. 1976. Proterosuchia. In: Kuhn, O. (ed.) Handbuch der Paläoherpetologie
- 710 13. Gustav Fischer, Stuttgart, 11–39.
- 711 Chatterjee S. 1985. Postosuchus, a new thecodontian reptile from the Triassic of Texas and the
- origin of tyrannosaurs. *Philosophical Transactions of the Royal Society of London B* **309**:395-
- 713 460.
- 714 Chen ZQ, Benton MJ. 2012. The timing and pattern of biotic recovery following the end-
- Permian mass extinction. *Nature Geoscience* **5(6)**:375-383.
- 716 Citton P, Ronchi A, Nicosia U, Sacchi E, Maganuco S, Cipriani A, Innamorati G, Zuccari
- 717 C, Manucci F, Romano M. 2020. Tetrapod tracks from the Middle Triassic of NW Sardinia
- 718 (Nurra region, Italy). *Italian Journal of Geosciences* **139(2)**:309-320.
- 719 Costamagna LG. 2013. Middle Triassic carbonate lithostratigraphy of the Southern
- 720 Briançonnais (Cottian Alps, Italy) and comparison with the surrounding areas. *GeoActa* 12:1-
- 721 24.
- 722 Costamagna LG, Barca S, Nervo R. 2002. Analisi di facies della successione carbonatica
- mediotriassica del Dominio Brianzonese fra le valli Stura e Maira (Alpi Occidentali, Cuneo,



- 724 Italia): La sezione del Vallone del Preit. In: Fioraso G., Malusà M., Mosca P. & Tallone S.
- 725 (eds.) 81<sup>a</sup> Riunione estiva SGI, Riassunti delle Comunicazioni orali e dei poster: 110-111,
- 726 Torino.
- 727 Courel L, Demathieu G. 1976. Une ichnofaune reptilienne remarquable dans les grès Triasique
- de Largentière (Ardèche, France). *Palaeontogr.* A 151: 194–216.
- 729 Courel L, Demathieu G, Gall JC. 1979. Figures sédimentaires et traces d'origine biologique du
- 730 Trias moyen de la bordure orientale du Massif Central. Signification sédimentologique et
- paleoécologique. *Geobios* **12**: 379-397.
- 732 Cruickshank ARI. 1972. The proterosuchian thecodonts. In: Joysey, K. A. & Kemp, T. S. (eds)
- Studies in Vertebrate Evolution. Oliver and Boyd, Edinburgh, 89–119.
- 734 Cruickshank ARI. 1978. The pes of Eythrosuchus africanus Broom. Zoological Journal of the
- 735 *Linnean Society* **62**:161-177.
- d'Atri A, Piana F, Barale L, Bertok C, Martire L. 2016. Geological setting of the southern
- termination of Western Alps. *International Journal of Earth Sciences* **105(6)**:1831-1858.
- 738 **Decarlis A, Lualdi A. 2009**. A sequence stratigraphic approach to a Middle Triassic shelf-slope
- complex of the Ligurian Alps (Ligurian Briançonnais, Monte Carmo-Rialto unit, Italy).
- 740 Facies **55**:267-290.
- 741 Decarlis A, Dallagiovanna G, Lualdi A, Maino M, Seno S. 2013. Stratigraphic evolution in the
- Ligurian Alps between Variscan heritages and the Alpine Tethys opening: A review. *Earth*-
- 743 *Science Reviews* 125:43-68.
- 744 Decarlis A, Manatschal G, Haupert I, Masini E 2015. The tectono-stratigraphic evolution of
- distal, hyper-extended magma-poor conjugate rifted margins: Examples from the Alpine
- 746 Tethys and Newfoundland–Iberia. *Marine and Petroleum Geology* **68**:54-72.



- 747 **Demathieu G. 1970**. Les empreintes de pas de vertébrés du Trias de la bordure Nord-Est du
- Massif Central. Cahiers de Paléontologie CRNS Paris, 211 p.
- **Demathieu G. 1984**. Une ichnofaune du Trias moyen du basin de Lodève (Hérault, France).
- 750 *Ann. Paleontol. (Vertebr.-Invertebr.)* **70:** 247-273.
- 751 **Demathieu G, Weidmann M. 1982**. Les empreintes de pas de reptiles dans le Trias du Vieux
- 752 Emosson (Finhaut, Valais, Suisse). *Eclogae Geologicae Helvetiae* **75**:721–757.
- 753 **Díaz-Martínez I, Pérez-García A. 201**2. Historical and comparative study of the first Spanish
- vertebrate paleoichnological record and bibliographic review of the Spanish chirotheriid
- 755 footprints. *Ichnos*, **19(3)**: 141-149.
- 756 Diaz-Martinez I, Castanera D, Gasca JM, Canudo JI. 2015. A reappraisal of the Middle
- 757 Triassic chirotherium ibericus Navas, 1906 (Iberian Range, NE Spain), with
- comments on the Triassic tetrapod track biochronology of the Iberian Peninsula. *PeerJ*
- **3**:1044.
- 760 **Diedrich C. 2015**. *Isochirotherium* trackways, their possible trackmakers (?*Arizonasaurus*):
- intercontinental giant archosaur migrations in the Middle Triassic tsunami-influenced
- carbonate intertidal mud flats of the European Germanic Basin. *Carbonates and Evaporites*
- **30**:229-252.
- 764 Egerton PG. 1839. On two casts in sandstone of impression of the Hind Foot of a gigantic
- 765 Cheirotherium, from the New red sandstone of Cheshire. The London and Edinburgh
- *Philosophical Magazine and Journal of Science, 3rd series* **14(75)**:151-158.
- 767 **Erwin DH. 1992**. A preliminary classification of evolutionary radiations. *Historical Biology*
- **6**:133–147.



- 769 Erwin DH. 1993. The Great Paleozoic Crisis, Life and Death in the Permian. Colombia
- University Press, New York, 327 pp.
- 771 Erwin DH. 2001. Lessons from the past: biotic recoveries from mass extinctions. *Proceedings of*
- the National Academy of Sciences **98(10)**:5399-5403.
- Evans SE, Wang Y. 2005. Dalinghosaurus, a lizard from the Early Cretaceous Jehol Biota of
- north- east China. *Acta Paleontologica Polonica* **50**:725-742.
- 775 Ezcurra MD. 2016. The phylogenetic relationships of basal archosauromorphs, with an
- emphasis on the systematics of proterosuchian archosauriforms. *PeerJ* 4:e1778.
- 777 Ezcurra MD, Butler RJ. 2015. Taxonomy of the proterosuchid archosauriforms (Diapsida:
- Archosauromorpha) from the earliest Triassic of South Africa, and implications for the early
- archosauriform radiation. *Palaeontology* **58(1)**:141-170.
- 780 Ezcurra MD, Butler RJ, Gower DJ. 2013. 'Proterosuchia': the origin and early history of
- 781 Archosauriformes. *Geological Society, London, Special Publications* **379(1)**:9-33.
- 782 Ezcurra MD, Gower DJ, Sennikov AG, Butler RJ. 2019. The osteology of the holotype of the
- early erythrosuchid *Garjainia prima* Ochev, 1958 (Diapsida: Archosauromorpha) from the
- value of the Linnean Society upper Lower Triassic of European Russia. Zoological Journal of the Linnean Society
- **185**:717–783.
- 786 Ezcurra MD, Jones AS, Gentil AR, Butler RJ. 2020. Early Archosauromorphs: The Crocodile
- and Dinosaur Precursors. Encyclopedia of Geology, 2nd edition.
- 788 Ezcurra MD, Velozo P, Meneghel M, Piñeiro G. 2015. Early archosauromorph remains from
- the Permo-Triassic Buena Vista Formation of north-eastern Uruguay. *PeerJ* **3**:e776.
- 790 Feldmann M, Furrer H, Glarus K. 2009. Die Saurierspuren am Tödi und ihre geologische
- 791 Umgebung. Mitteilungen der Naturforschenden Gesellschaft des Kantons Glarus 18:28-37.



Fortuny J, Bolet A, Selles AG, Cartanya J, Galobart A. 2011. New insights on the Permian 792 and Triassic vertebrates from the Iberian peninsula with emphasis on the Pyrenean and 793 Catalonian basins. *Journal of Iberian Geology* **37(1)**:65-86. 794 Gand G. 1978. Interprétations paléontologique et paléoècologique d'un sixième assamblage à 795 traces de reptiles des carrières triasiques de St.-Sernin-du Bois (Autunois, France). 796 797 Conclusions gènèrales à ètude du gisement. Bulletin de la Société d'Historie Naturelle d'Autun 87: 9–29. 798 Gand G. 1979. Description de deux nouvelles traces d'Isochirotherium observées dans les grès 799 du Trias moyen de Bourgogne. Bull. Soc. Hist. Nat. Creusot 37: 13-25. 800 Gidon M. 1958a. Nouvelles observations sur la zone brianconnaise au delà de la frontière 801 franco-italienne (Bassin de la Haute Maira, Province de Cuneo). Trav. Lab. Géol. Univ. 802 *Grenoble* **34**:153-167. 803 Gidon M. 1958b. La Zone Briançonnaise en Haute Ubaye (Basses-Alpes) et son prolongement 804 au Sud-Est. PhD Thesis. Faculté des Sciences de l'Université de Grenoble, 272 pp. 805 Gidon M. 1972. Les chainons brianconnais et subbrianconnais de la rive gauche de la Stura 806 entre la Val de l'Arma (province de Cuneo-Italie). Géologie Alpine 48(1):87-120. 807 Gidon M. 1978. Carte géologique détaillée de la France à l'échelle 1/50.000, feuille Larche, 1° 808 édition. Bureau de Recherche Géologique et Minière, Orléans, with explanatory notes, pp. 1– 809 28. 810 811 Golden Software 2002. Surfer version 8.0: surface mapping system. Gottmann-Quesada A, Sander PM. 2009. A redescription of the early archosauromorph 812 Protorosaurus speneri Meyer, 1832 and its phylogenetic relationships. Palaeontographica 813 814 Abteilung A **287**:123-220.



- 815 Gower DJ. 1996. The tarsus of erythrosuchid archosaurs, and implications for early diapsid
- phylogeny. *Zoological Journal of the Linnean Society* **116(4)**:347-375.
- **Gower DJ. 2003**. Osteology of the early archosaurian reptile *Erythrosuchus africanus* Broom.
- Annals of the South African Museum 110:1-88.
- 819 Gower DJ, Sennikov AG. 2000. Early Archosaurs from Russia. In: Benton MJ, Shishkin MA,
- 820 Unwin DM, Kurochkin EN, editors. The Age of Dinosaurs in Russia and Mongolia.
- Cambridge University Press, Cambridge. pp. 140–159.
- 822 Gower DJ, Hancox PJ, Botha-Brink J, Sennikov AG, Butler RJ. 2014. A new species of
- 623 *Garjainia* Ochev, 1958 (Diapsida: Archosauriformes: Erythrosuchidae) from the Early
- Triassic of South Africa. *PLoS One* **9(11)**:e111154.
- 825 Grasby SE, Sanei H, Beauchamp B. 2011. Catastrophic dispersion of coal fly ash into oceans
- during the latest Permian extinction. *Nature Geoscience* **4(2)**:104.
- 827 **Hallam A. 1991**. Why was there a delayed radiation after the end-Palaeozoic extinctions?.
- 828 *Historical Biology* 5(2-4):257-262.
- Haubold H, Klein H. 2002. Chirotherien und Grallatoriden aus der Unteren bis Oberen Trias
- Mitteleuropas und die Entstehung der Dinosauria. *Hallesches Jahrbuch für*
- 831 *Geowissenschaften B* **24**:1-22.
- Haubold H. 1967. Eine Pseudosuchier- Fährtenfauna aus dem buntsandstein südthüringens.
- Hallesches Jahrbuch für Mitteldeutsche Erdgeschichte **8**:12-48.
- Haubold H. 1984. Saurierfährten. A. Ziemsen Verlag, Wittenberg, 232 pp.
- Haubold H. 1971a. Die Tetrapodenfährten des Buntsandsteins. Paläontologische Abhandlungen
- 836 *A* **4(3)**:395-548.



- 837 Haubold H. 1971b. Ichnia Amphibiorum et Reptiliorum fossilium. Encyclopedia of
- Paleoherpetology **18**:1-124.
- Haubold H. 1970. Die Tetrapodenfährten des Germanischen Buntsandsteins und ihre
- Äquivalente in der gesamten Trias. *Paläontologische Abhandlungen, Abteilung A,*
- 841 Palaeozoologie, 4.
- Haubold H. 1984. Saurierfährten. Wittenberg, Ziemsen, 231 p.
- Haubold H. 1986. Archosaur footprints at the terrestrial Triassic–Jurassic transition. 190–201.
- In Padian K. (ed.). The beginning of the Age of Dinosaurs: Faunal change across the Triassic–
- Jurassic boundary. Cambridge University Press, Cambridge, 378 pp.
- Haubold H. 2006. Die Saurierfährten *Chirotherium barthii* Kaup, 1835—das Typusmaterial aus
- dem Buntsandstein bei Hildburghausen/Thüringen und das Chirotherium-Monument.
- *Veröffentlichungen Naturhistorisches Museum Schleusingen* **21**:3–31.
- Huene F. von 1902. Übersichtüber die Reptilien der Trias. Geologische und Paläontologische
- *Abhandlungen* **10**:1-84.
- Joachimski MM, Lai X, Shen S, Jiang H, Luo G, Chen B, Chen J, Sun Y. 2012. Climate
- warming in the latest Permian and the Permian–Triassic mass extinction. *Geology* **40**:195–
- 853 198.
- Kaup JJ. 1835. Über Tierfährten bei Hildburghausen. Neues Jahrbuch für Mineralogie,
- *Geologie und Paläontologie* 1835, 327–328.
- 856 Kidder DL, Worsley TR. 2004. Causes and consequences of extreme Permo–Triassic warming
- to globally equable climate and relation to the Permo–Triassic extinction and recovery.
- 858 Palaeogeography, Palaeoclimatology, Palaeoecology **203(3–4)**:207–237.



359	King MJ, Sarjeant WAS, Thompson DB, Tresise G. 2005. A revised systematic
360	ichnotaxonomy and review of the vertebrate footprint ichnofamily Chirotheriidae from the
361	British Triassic. Ichnos 12:241-299.
362	Klein H, Lucas SG. 2010a. Tetrapod footprints and their use in biostratigraphy and
363	biochronology of the Triassic. In Lucas, S.G. (ed.), The Triassic timescale. Geological Society
364	of London Special Publications <b>334</b> :419-446.
365	Klein H, Niedźwiedzki G. 2012. Revision of the Lower Triassic tetrapod ichnofauna from
366	Wióry, Holy Cross Mountains, Poland. New Mexico Museum of Natural History and Science,
367	Bulletin <b>56</b> :1-62.
368	Klein H, Haubold H. 2007. Archosaur footprints-potential for biochronology of Triassic
369	continental sequences. New Mexico Museum of Natural History and Science Bulletin 41:120-
370	130.
371	Klein H, Lucas SG. 2010. Review of the tetrapod ichnofauna of the Moenkopi Formation/Group
372	(Early-Middle Triassic) of the American Southwest. New Mexico Museum of Natural History
373	and Science Bulletin <b>50</b> :1-67.
374	Klein H, Voigt S, Hminna A, Saber H, Schneider J, Hmich D. 2010. Early Triassic archosaur
375	dominated footprint assemblage from the Argana Basin (western High Atlas, Morocco).
376	Ichnos 17(3):215-227.
377	Klein H, Voigt S, Saber H, Schneider JW, Hminna A, Fischer J, Lagnaoui A, Brosig A.
378	2011. First occurrence of a Middle Triassic tetrapod ichnofauna from the Argana Basin
379	(Western High Atlas, Morocco). Palaeogeography, Palaeoclimatology, Palaeoecology
380	<b>307</b> :218-231.



881	Klein H, Wizevich MC, Thuring B, Marty D, Thuring S, Falkingham P, Meyer CA. 2016.
882	Triassic chirotheriid footprints from the Swiss Alps: ichnotaxonomy and depositional
883	environment (Cantons Wallis & Glarus). Swiss Journal of Palaeontology, 135(2): 295-314.
884	Knoll AH, Bambach RK, Payne JL, Pruss S, Fischer WW. 2007. Paleophysiology and end-
885	Permian mass extinction. Earth and Planetary Science Letters 256(3-4):295-313.
886	Krainer K, Lucas SG, Ronchi A. 2012. Tetrapod footprints from the Alpine Buntsandstein
887	(Lower Triassic) of the Drau Range (Eastern Alps, Austria). Jahrbuch der Geologischen
888	Bundesanstalt <b>152</b> :205-212.
889	Krebs B. 1965. Die Triasfauna der Tessiner Kalkalpen, XIX. Ticinosuchus ferox nov. gen. nov.
890	sp. Schweizerische Paläontologische Abhandlungen <b>81</b> :1-140.
891	Kubo T, Benton MJ. 2007. Evolution of hindlimb posture in archosaurs: limb stresses in extinct
892	vertebrates. Palaeontology 50(6):1519-1529.
893	Kubo T, Benton MJ. 2009. Tetrapod postural shift estimated from Permian and Triassic
894	trackways. Palaeontology 52(5):1029-1037.
895	Lautenschlager S, Desojo JB. 2011. Reassessment of the Middle Triassic rauisuchian
896	archosaurs Ticinosuchus ferox and Stagonosuchus nyassicus. Paläontologische Zeitschrift
897	<b>85(4)</b> : 357-381.
898	Leonardi G. 1987. Glossary and manual of tetrapod footprint palaeoichnology. p.p. 117.
899	Brasilia: Ministerio das Minas e Energia Departamento Nacional da Producao Mineral.
900	Lorenzoni S, Zanettin E. 1958. Contributo alla conoscenza del giacimento uranifero di Preit
901	(Alpi Cozie). Studi e Ricerche Divisione Geomineraria CNRN 1(2):349-433.



- 902 Lualdi A, Bianchi U. 1990. La Formazione di Costa Losera: una nuova unità stratigrafica
- dell'Anisico delle Alpi Liguri. *Atti Ticinensi di Scienze della Terra* **33**:33-62.
- 904 Lualdi A, Seno S. 1984. Osservazioni stratigrafiche e tettoniche nella zona dei Rio di Nava
- 905 (Brianzonese Ligure Esterno, Unità di Ormea). Memorie della Società Geologica Italiana
- **28**:493-503.
- 907 Malaroda R. 1970. Carta geologica del Massiccio dell'Argentera alla scala 1: 50.000. Allegato
- 908 al vol. 9 delle Memorie della Società Geologica Italiana.
- 909 Mallison H, Wings O. 2014. Photogrammetry in paleontology—a practical guide. *Journal of*
- 910 *Paleontological Techniques* **12**:1-31.
- 911 Manning PL. 2004. A new approach to the analysis and interpretation of tracks: examples from
- 912 the dinosauria. *Geological Society, London, Special Publications*, **228(1)**: 93-123.
- 913 Megard-Galli J, Baud A. 1977. Le Trias moyen et supérieur des Alpes nord-occidentales et
- occidentales: données nouvelles et corrélations stratigraphiques. Bulletin B.R.G.M. 4(3):233-
- 915 250.
- 916 Melchor RN, De Valais S. 2006. A review of Triassic tetrapod track assemblages from
- 917 Argentina. *Palaeontology* **49(2)**:355-379.
- 918 Motani R, Jiang DY, Chen GB, Tintori A, Rieppel O, Ji C, Huang JD. 2015a. A basal
- 919 ichthyosauriform with a short snout from the Lower Triassic of China. *Nature* **517(7535)**:485-
- 920 488.
- 921 Motani R, Jiang DY, Tintori A, Rieppel O, Chen GB, You H. 2015b. Status of Chaohusaurus
- 922 chaoxianensis (Chen, 1985). Journal of Vertebrate Paleontology **35(1)**:e892011.
- Nesbitt SJ. 2011. The early evolution of archosaurs: relationships and the origin of major clades.
- 924 Bulletin of the American Museum of Natural History 41(supp.):1-292.



925	Nesbitt SJ, Liu J, Li C. 2010. A sail-backed suchian from the Heshanggou Formation (Early
926	Triassic: Olenekian) of China. Earth and Environmental Science Transactions of the Royal
927	Society of Edinburgh 101:271–284.
928	Olsen PE. 1995. A new approach for recognizing track makers. Geological Society of America,
929	Abstracts with Programs 27:72.
930	Olsen PE, Smith JB, McDonald NG. 1998. Typematerial of the type species of the classic
931	theropod footprint genera Eubrontes, Anchisauripus and Grallator (Early Jurassic, Hartford
932	and Deerfield basins, Connecticut and Massachusetts, U.S.A.). J. Vertebr. Paleontol. 18: 586-
933	601.
934	Payne JL, Lehrmann DJ, Wei J, Orchard MJ, Schrag DP, Knoll AH. 2004. Large
935	perturbations of the carbon cycle during recovery from the end-Permian extinction. Science
936	<b>305</b> :506-509.
937	Payne JL, Summers M, Rego BL, Altiner D, Wei J, Yu M, Lehrmann DJ. 2011. Early and
938	Middle Triassic trends in diversity, evenness, and size of foraminifers on a carbonate platform
939	in south China: implications for tempo and mode of biotic recovery from the end-Permian
940	mass extinction. Paleobiology 37:409-425.
941	Peabody FE. 1948. Reptile and amphibian trackways from the Lower Triassic Moenkopi
942	formation of Arizona and Utah. Bulletin of the Department of Geological sciences 27:295-
943	468.
944	Peecook BR, Smith RM, Sidor CA. 2018. A novel archosauromorph from Antarctica and an
945	updated review of a high-latitude vertebrate assemblage in the wake of the end-Permian mass
946	extinction. Journal of Vertebrate Paleontology 38(6):e1536664.



947	Petti FM, Avanzini M, Belvedere M, De Gasperi M, Ferretti P, Girardi S, Remondino F,
948	Tomasoni R. 2008. Digital 3D modelling of dinosaur footprints by photogrammetry and laser
949	scanning techniques: integrated approach at the Coste dell'Anglone tracksite (Lower Jurassic,
950	Southern Alps, Northern Italy). Studi Trentini di Scienze Naturali, Acta Geologica 83:303-
951	315.
952	Petti FM, Bernardi M, Kustatscher E, Renesto S, Avanzini M. 2013. Diversity of continental
953	tetrapods and plants in the Triassic of the Southern Alps: Ichnological, paleozoological and
954	paleobotanical evidence. In Tanner, L.H., Spielmann, J.A. and Lucas, S.G. (eds.), The
955	Triassic System. New Mexico Museum of Natural History and Science, Bulletin 61:458-484.
956	Peyer K, Carter JG, Sues H-D, Novak SE, Olsen PE. 2008. A new suchian archosaur from the
957	Upper Triassic of North Carolina. Journal of Vertebrate Paleontology 28:363-381.
958	Pough FH, Heiser JB, McFarland WN. 1996. Vertebrate Life. Prentice Hall International, New
959	Jersey.
960	Racki G. 2003. End-Permian mass extinction: oceanographic consequences of double
961	catastrophic volcanism. <i>Lethaia</i> <b>35</b> :171–173.
962	Racki G, Wignall PB. 2005. Late Permian double-phased mass extinction and volcanism: an
963	oceanographic perspective. In: Over, D.J., Morrow, J.R., Wignall, P.B. (Eds.), Understanding
964	Late Devonian and Permian-Triassic Biotic and Climatic Events: Towards an Integrated
965	Approach. Elsevier B.V., pp. 263–297.
966	Remondino F, Rizzi A, Girardi S, Petti FM, Avanzini M. 2010. 3D Ichnology—recovering
967	digital 3D models of dinosaur footprints. The Photogrammetric Record 25(131):266-282.
968	Retallack GJ. 2005. Permian greenhouse crises. The nonmarine Permian. New Mexico Museum
969	of Natural History and Science Bulletin <b>30</b> :256-269.



- 970 **Retallack GJ. 2009**. Greenhouse crises of the past 300 million years. *Geological Society of*
- 971 *America Bulletin* **121(9-10)**:1441-1455.
- 972 **Retallack GJ. 2013**. Permian and Triassic greenhouse crises. *Gondwana Research* **24(1)**:90-103.
- 973 Retallack GJ, Jahren AH. 2008. Methane release from igneous intrusion of coal during Late
- Permian extinction events. *The Journal of Geology* **116**:1–20.
- 975 Retallack GJ, Sheldon ND, Carr PF, Fanning M, Thompson CA, Williams ML, ... Hutton
- 976 **A. 2011**. Multiple Early Triassic greenhouse crises impeded recovery from Late Permian
- mass extinction. *Palaeogeography*, *Palaeoclimatology*, *Palaeoecology* **308(1–2)**:233–251.
- 978 Romano M, Citton P, Nicosia U. 2015. Corroborating trackmaker identification through
- 979 footprint functional analysis: the case study of *Ichniotherium* and *Dimetropus*. Lethaia
- **49**:102-116.
- 981 Romer AS. 1971. The Chanares (Argentina) Triassic reptile fauna XI. Two new long-snouted
- thecodonts, *Chanaresuchus* and *Gualosuchus*. Breviora **379**:1-22.
- 983 Santi G, Lualdi A, Decarlis A, Nicosia U, Ronchi A. 2015. Chirotheriid footprints from the
- Lower-Middle Triassic of the Briançonnais Domain (Pelite di Case Valmarenca, Western
- 985 Liguria, NW Italy). Bollettino della Società Paleontologica Italiana 54(2):82.
- 986 Scheyer TM, Romano C, Jenks J, Bucher H. 2014. Early Triassic marine biotic recovery: the
- predators' perspective. *PLoS ONE* **9**:e88987.
- 988 Sephton MA, Looy CV, Brinkhuis H, Wignall PB, de Leeuw JW, Visscher H. 2005.
- 989 Catastrophic soil erosion during the end–Permian biotic crisis. *Geology* **33**:941–944.
- 990 **Sereno PC. 1991**. Basal archosaurs: phylogenetic relationship and functional implications.
- 991 *Journal of Vertebrate Paleontology* **11**:1–53.



Shen J, Chen J, Algeo TJ, Yuan S, Feng Q, Yu J, ... Planavsky NJ. 2019. Evidence for a 992 prolonged Permian-Triassic extinction interval from global marine mercury records. Nature 993 communications 10(1):1563. 994 Schmid SM, Fügenschuh B, Kissling E, Schuster R. 2004. Tectonic map and overall 995 architecture of the Alpine orogen. Eclogae Geologicae Helvetiae 97:93-117. 996 Schmid SM, Kissling E, Diehl T, van Hinsbergen DJJ, Molli G. 2017. Ivrea mantle wedge, 997 arc of the Western Alps, and kinematic evolution of the Alps - Apennines orogenic system. 998 Swiss Journal of Geosciences 110:581-612. 999 1000 Schobben M, Joachimski MM, Korn D, Leda L, Korte C. 2014. Palaeotethys seawater temperature rise and an intensified hydrological cycle following the end-Permian mass 1001 extinction. Gondwana Research 26:675-683. 1002 1003 Sepkoski JJ Jr. 1984. A kinetic model of Phanerozoic taxonomic diversity. III. Post–Paleozoic families and mass extinctions. *Paleobiology* **10**:246–267. 1004 Smith RMH, Evans SE. 1996. New material of *Youngina*: evidence of juvenile aggregation in 1005 Permian diapsid reptiles. *Palaeontology* **39**:289-303. 1006 Song H, Wignall PB, Tong J, Yin H. 2013. Two pulses of extinction during the Permian— 1007 1008 Triassic crisis. *Nature Geoscience* **6(1)**:52. Song H, Wignall PB, Tong J, Song H, Chen J, Chu D, ... Lai X. 2015. Integrated Sr isotope 1009 variations and global environmental changes through the Late Permian to early Late Triassic. 1010 1011 Earth and Planetary Science Letters **424**:140–147. Sookias RB, Butler RJ. 2013. Euparkeriidae. Geological Society, London, Special Publications 1012 **379**:35-48. 1013 1014 Sues HD, Desojo JB, Ezcurra MD. 2013. Doswelliidae: a clade of unusual armoured



1037

archosauriforms from the Middle and Late Triassic. Geological Society, London, Special 1015 Publications 379:SP379-13. 1016 Sun Y, Joachimski M, Wignall PB, Yan C, Chen Y, Jiang H, Wang L, Lai X. 2012. Lethally 1017 Hot Temperatures During the Early Triassic Greenhouse. Science 338:1-35. 1018 Torsvik TH, Van Der Voo R, Preeden U, Mac C, Steinberger B, Doubrovine PV, van 1019 Hinsbergen DJJ, Domeier M, Gaina C, Tohver E, Meert JG, McCausland PJA, Cocks 1020 LRM. 2012. Earth-Science Reviews Phanerozoic polar wander, palaeogeography and 1021 dynamics. Earth Science Reviews 114(3-4):325-368. 1022 1023 Treasise G, Sarjeant WAS. 1997. The tracks of Triassic Vertebrates. Fossil Evidence from North-West England. The stationery Office, London, 204 pp. 1024 Trotteyn MJ, Arcucci AB, Raugust T. 2013. Proterochampsia: an endemic archosauriform 1025 1026 clade from South America. In: Anatomy, Phylogeny and Palaeobiology of Early Archosaurs and their Kin (eds Nesbitt S.J., Desojo J.B., Irmis R.B.), Geological Society, London, Special 1027 Publications **379**:59–90. 1028 Van Hinsbergen DJJ, De Groot LV, Van Schaik SJ, Spakman W, Bijl PK, Sluijs A, 1029 **Langereis CG, Brinkhuis H. 2015**. A paleolatitude calculator for paleoclimate studies. *PLoS* 1030 1031 *ONE* **10(6)**:1-21. Vanossi M. 1969. La serie brianzonese di Salto del Lupo (Liguria Occ.): osservazioni 1032 sedimentologico-stratigrafiche. Atti Ist. Geol. Univ. Pavia 20: 3-16. 1033 1034 Vanossi M. 1974. L'Unità di Ormea: una chiave per l'interpretazione del Brianzonese ligure. Tipografia del libro. 1035 Vanossi M. 1991. Guide Geologiche Regionali, 11 itinerari, Alpi Liguri (a cura della SGI), 296 1036

pp. BE-MA Edit., Milano.



1038	Welles SP. 1947. Vertebrates from the Upper Moenkopi Formation of Northern Arizona.
1039	University of California Publications in Geological Science 27:241-294.
1040	Whiteside JH, Ward PD. 2011. Ammonoid diversity and disparity track episodes of chaotic
1041	carbon cycling during the early Mesozoic. <i>Geology</i> <b>39</b> :99–102.
1042	Wignall PR. 2001. Large igneous provinces and mass extinctions. Earth-Science Reviews 53:1
1043	33.
1044	Wilson JA 2005. Integrating ichnofossil and body fossil records to estimate locomotor posture
1045	and spatiotemporal distribution of early sauropod dinosaurs: a stratocladistic approach.
1046	Paleobiology <b>31(3)</b> : 400-423.
1047	Withers PC. 1992. Comparative Animal Physiology. Saunders College, New York.
1048	Xing LD, Klein H, Lockley MG, Li J, Zhang J, Matsukawa M, Xiao J. 2013. Chirotherium
1049	trackways from the Middle Triassic of Guizhou, China. <i>Ichnos</i> <b>20</b> :99–107.
1050	Young CC. 1964. The pseudosuchians in China. <i>Palaeontologia Sinica Series C</i> 19:105-205.
1051	Zhang F. 1975. A new thecodont Lotosaurus, from Middle Triassic of Hunan. Vertebrata
1052	PalAsiatica <b>13</b> :144-147.
1053	Ziegler PA, Stampfli GM. 2001. Late Palaeozoic-Early Mesozoic plate boundary
1054	reorganization: collapse of the Variscan orogen and opening of Neotethys. In: Cassinis G.
1055	(Ed.), Permian Continental Deposits of Europe and Other Areas. Regional Reports and
1056	Correlations. Annali Museo Civico Scienze Naturali, Brescia 25:17–34.
1057	
1058	Figure captions
1059	



1060	Fig. 1 - Geologic map of the Pianezza area. In the upper row the location of Maira Valley and
1061	Gardetta-Pianezza area. For the geologic map: 1= volcanic complex and graphitic schist
1062	(upper Carboniferous - Permian); 2= conglomerate, 3= quartz-conglomerate, and 4= quartz-
1063	arenite and quartz-siltite of the quartzitic complex (upper Permian - early Lower Triassic); 5=
1064	lower carniole complex (late Lower Triassic); 6= lower calcareous complex (lower Anisian -
1065	early upper Ladinian); 7= upper dolomitic complex (upper Ladinian); 8= lakes and peat bog;
1066	9= faults; 10= location of the footprint site; in white the detritic cover and moraines.
1067	Fig. 2 - Correlation scheme among the Briançonnais s.s., the Ligurian Briançonnais, from De
1068	Carlis & Lualdi, 1990 redrawn and modified. PNQ: "Ponte di Nava Quartzites", CVP: Case
1069	Val Marenca Pelites. The footprint silohuette marks the position of the track-bearing horizon.
1070	Fig. 3 – a) Panoramic view of the track surface with the line-drawing of the chirotherian
1071	trackways. In pale yellow the above-lying bed characterized by symmetric wave ripples; b)
1072	Detailed view of the GT-1 and GT-2 trackways, highlighted with the black colour.
1073	Fig. 4 – <i>Isochirotherium gardettae</i> ichnosp. nov. The GT-7 trackway, made of three consecutive
1074	manus-pes couples, is here highlighted by the red chalk and preserved in the upper track-
1075	bearing surface. Scale bar: 13 cm.
1076	Fig. 5 – a) <i>Isochirotherium gardettae</i> ichnosp. nov. Colour-coded and contour line image of the
1077	GT-7 trackway; b) Interpretative drawing of the GT-7 trackway.
1078	Fig. 6 – Reconstruction of the trackmaker's fore- and hind limbs, based on the 3D model and its
1079	interpretative drawing. Dashed lines define the metatarsal of digit V held lifted off the ground
1080	during locomotion.



Fig. 7 – Pentadactyl tracks from the Lower and Middle Triassic, assigned to the ichnogenus 1081 Chirotherium and their comparison with the studied tracks of the Gardetta ichnosite: a) GT-1-1082 3; b) GT-2-3; c) GT-2-8; d) GT-2-6; e), f) Chirotherium barthiii pes manus sets from type 1083 surface of the "Thüringischer Chirotheriensandstein", Hildburghausen, Germany; g) 1084 Chrotherium barthiii pes manus set from the Holbrook Member of the Moenkopi Formation 1085 (Middle Triassic), southwest of Cameron, northern Arizona; h) Chirotherium vorbachi pes 1086 manus set from the Lower Triassic of Aura an der Saale, Germany; i), Chirotherium sickleri 1087 "Thüringischer Chirotheriensandstein", Germany; 1), m) Chirotherium sickleri pes manus 1088 1089 sets from the Wupatki Member of the Moenkopi Formation (Lower Triassic), Meteor Crater, Arizona. Scale bar 10 cm. 1090 Fig. 8 - Pentadactyl tracks from the Lower and Middle Triassic, assigned to the ichnogenus 1091 *Isochirotherium* and their comparison with the studied tracks of the Gardetta ichnosite: a), b), 1092 c), pes manus sets of the GT-7 trackway; d) GT-3 isolated pes imprints of the lower track 1093 surface; e) Isochirotherium herculis pes manus set from the "Thüringischer 1094 Chirotheriensandstein" (Lower Triassic), Germany; f) *Isochirotherium marshalli* pes manus 1095 set from the Holbrook Member of the Moenkopi Formation (Middle Triassic), Penzance, 1096 1097 Northern Arizona; g) *Isochirotherium inferni* manus pes set from the Middle Triassic (late Anisian) of Adige Valley, Bolzano, Italy; h) *Isochirotherium coltoni* pes manus set from the 1098 Wupatki Member of the Moenkopi Formation (Lower Triassic), Meteor Crater, Arizona; i) 1099 1100 Isochirotherium lomasi pes manus set from the Middle Triassic (Anisian) of Cheshire, Great Britain; 1) *Isochirotherium coureli* pes manus set from the Middle Triassic (Anisian-Ladinian) 1101 of the Massif Central, France; m) *Isochirotherium hessbergense* pes manus set from the 1102 "Thüringischer Chirotheriensandstein" (Lower Triassic), Germany; n) Isochirotherium 1103



1104	demathieui pes manus set from the Middle Triassic of Mont d'Or Lyonnais, France; o)
1105	Isochirotherium soergeli pes manus set from the "Thüringischer Chirotheriensandstein"
1106	(Lower Triassic), Germany. Scale bar 10 cm.
1107	Fig. 9 – Fore- and hind-limb skeletons of Triassic archosauriforms and of the <i>Isochirotherium</i>
1108	gardettae trackmaker. Reconstructed right pes and manus skeletons of a) the Isochirotherium
1109	gardettae trackmaker in anterior/dorsal view; b) Postosuchus kirkpatricki CHATTERJEE 1985,
1110	USA, Norian; c) Postosuchus alisonae, PEYER et al. 2008, USA, Norian; d) Lotosaurus
1111	adentus ZHANG, 1975, China, Ladinian; e) Proterosuchus fergusi BROOM 1903, South Africa,
1112	Induan-?early Olenekian f) Erythrosuchus africanus BROOM 1905, South Africa, early
1113	Anisian; g) Shansisuchus shansisuchus Young 1964, China, late Anisian; h) Euparkeria
1114	capensis Broom, 1913, South Africa, Anisian; i) Chanaresuchus bonapartei ROMER, 1971,
1115	Argentina, Ladinian. Scale bars: a), b), c), d), f) $g$ = 10 cm; e), h) and i) = 1 cm.
1116	Fig. 10 – Life appearance of the non-archosaurian archosauriform (?Erythrosuchid) the most
1117	suitable producer of Isochirotherium gardettae. Simplified reconstruction of fore and hind
1118	autopodials in bottom (a) view. Complete life reconstruction in bottom (b), back (c), frontal
1119	(d) and lateral view (e) of the trackmaker. The gait and fore- and hind limbs were
1120	reconstructed according to the pattern and morphologies of GT-7 trackway (artwork by the
1121	Italian artist Fabio Manucci). See the supplementary video to get a more complete view of the
1122	reconstruction.
1123	Fig. 11 – Paleogeographic distribution of Early Triassic archosauriform footprints (yellow stars)
1124	and body fossil localities across Pangea. Black square = indeterminate archosauromorphs, red
1125	circles = non-archosauriform archosauromorphs, blue stars = archosauriforms. The
1126	palaeolatitude estimate for the southern Briançonnais domain is 11.8 N in the Olenekian (250



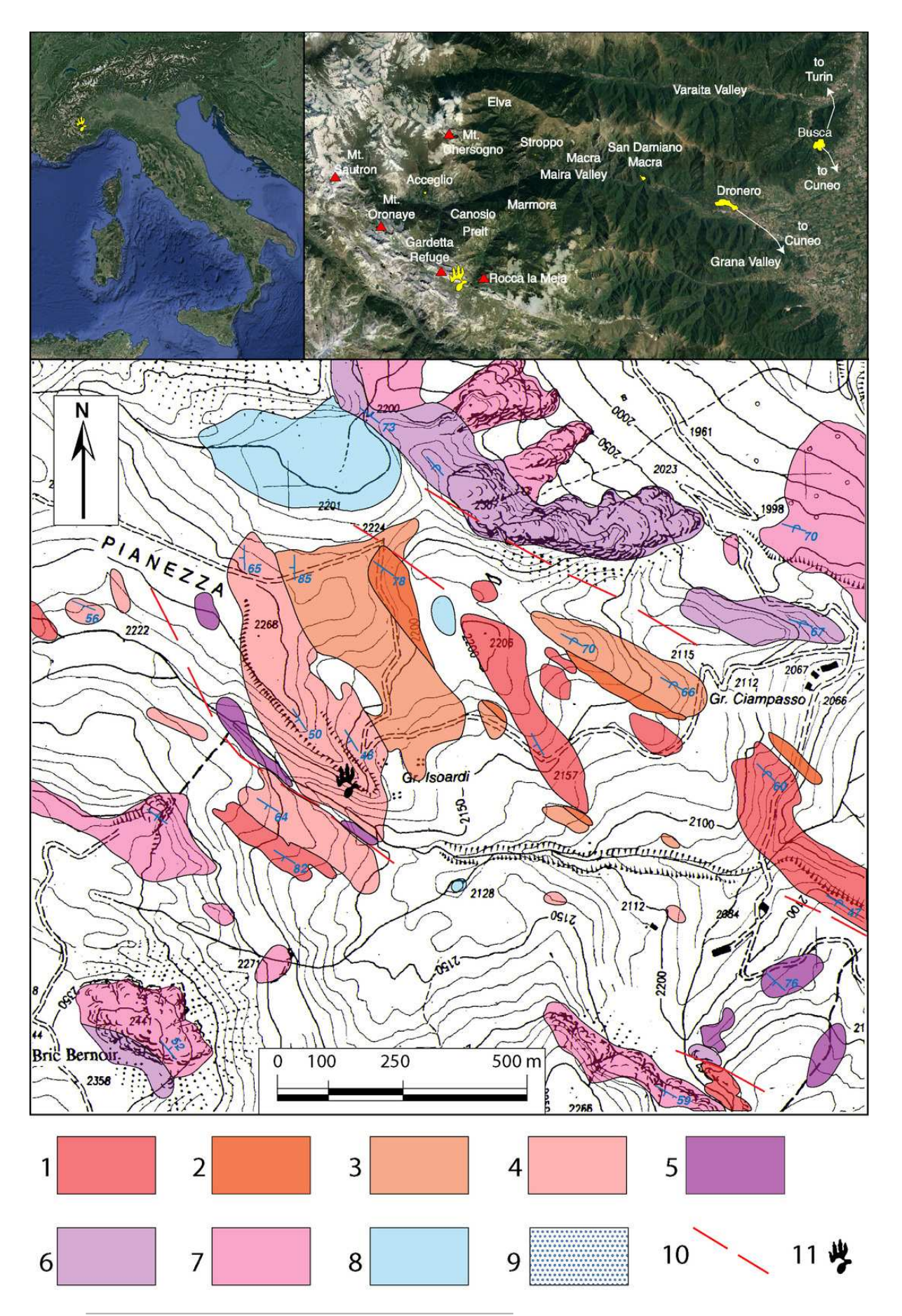
#### **PeerJ**

1127	Ma), confirming that archosauriforms were distributed also at low latitudes, in the tropical
1128	humid climatic belt. ImagePaleomap for 250 Ma downloaded from Fossilworks using data
1129	from the Paleobiology Database (Alroy, 2003). Redrawn and modified from Bernardi et al.,
1130	2015 and Benton (2018).
1131	



Geologic map of the Pianezza area

**Fig. 1** - Geologic map of the Pianezza area. In the upper row the location of Maira Valley and Gardetta-Pianezza area. For the geologic map: (1) volcanic complex and graphitic schist (upper Carboniferous - Permian). (2) Conglomerate. (4) Quartz-conglomerate, and quartz-arenite and quartz-siltite of the quartzitic complex (upper Permian - early Lower Triassic). (5) Lower carniole complex (late Lower Triassic). (6) Lower calcareous complex (lower Anisian - early upper Ladinian). (7) Upper dolomitic complex (upper Ladinian). (8) Lakes and peat bog. (9) Faults. (10) Location of the footprint site. In white the detritic cover and moraines.

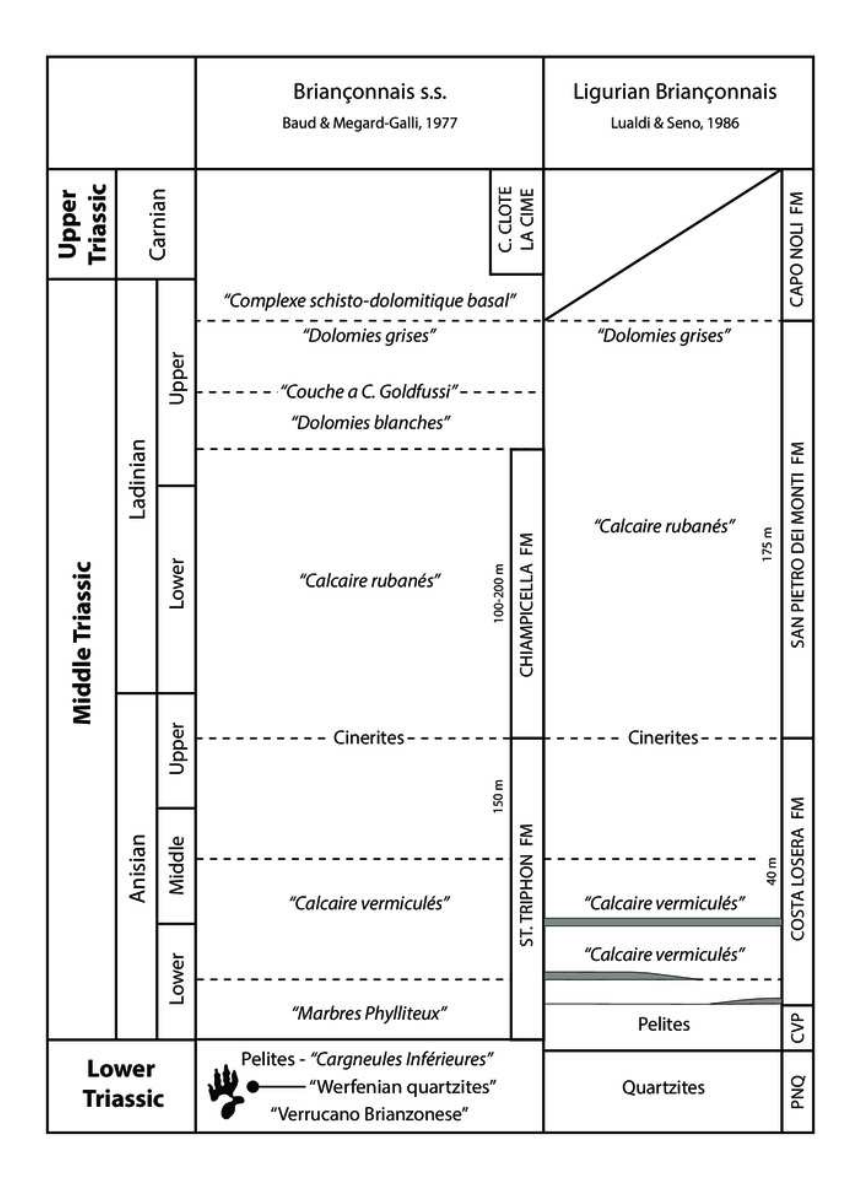




Correlation scheme among the Briançonnais s.s., the Ligurian Briançonnais

**Fig. 2** - Correlation scheme among the Briançonnais s.s., the Ligurian Briançonnais, from De Carlis & Lualdi, 1990 redrawn and modified. (PNQ) "Ponte di Nava Quartzites". (CVP) Case Val Marenca Pelites. The footprint silohuette marks the position of the track-bearing horizon.

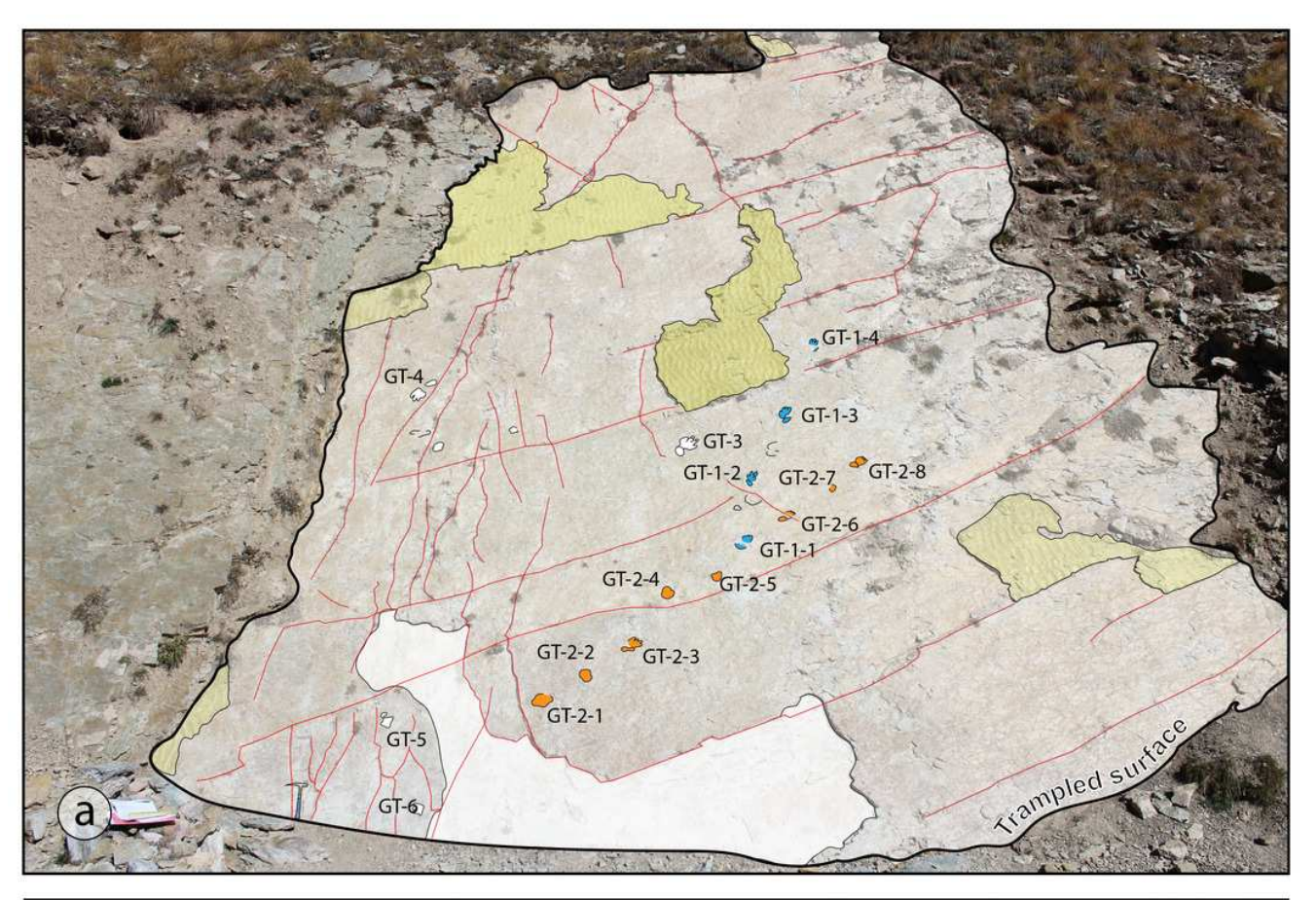






Panoramic view of the track surface with the line-drawing of the chirotherian trackways

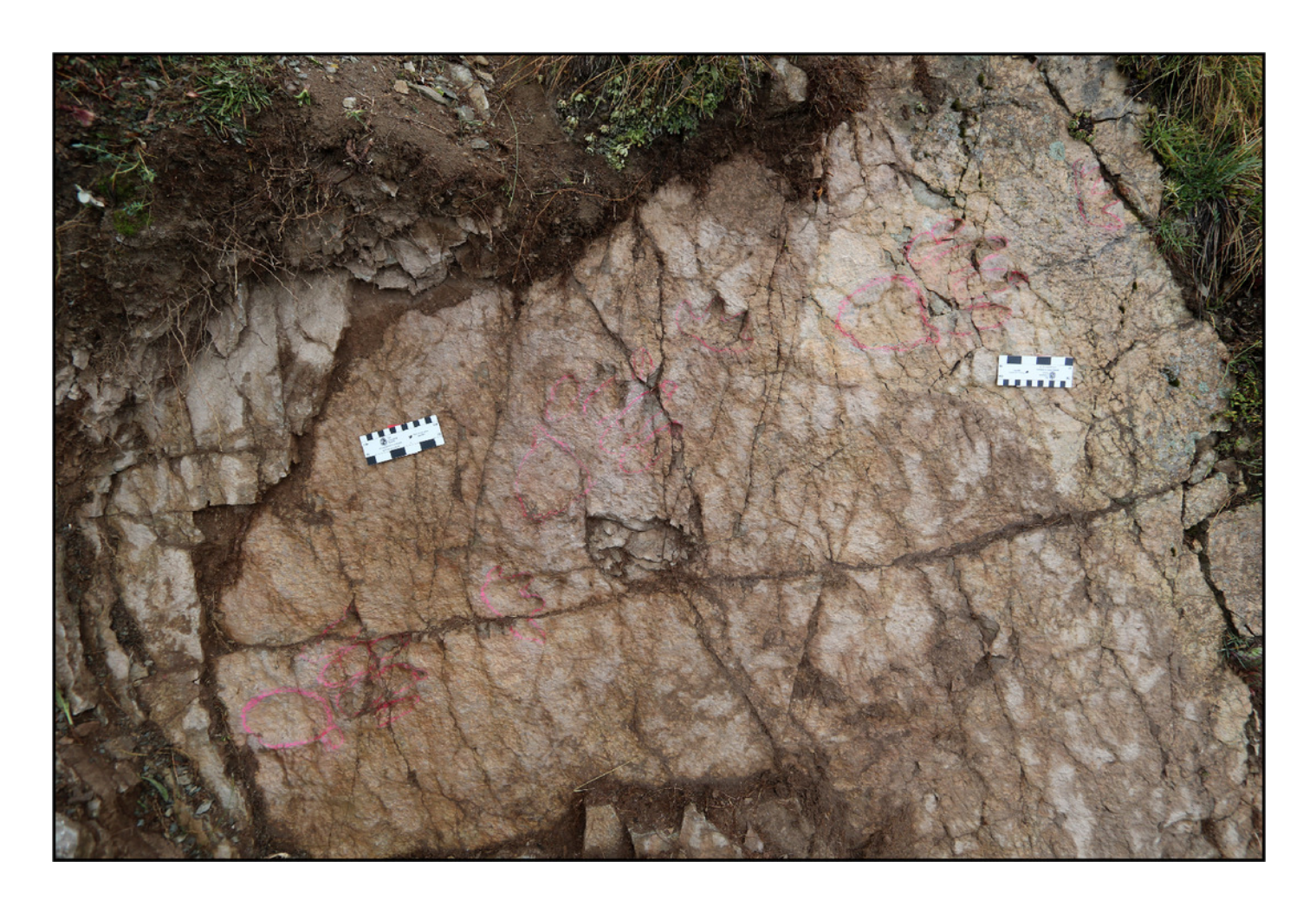
**Fig. 3** – (a) Panoramic view of the track surface with the line-drawing of the chirotherian trackways. In pale yellow the above-lying bed characterized by symmetric wave ripples. (b) Detailed view of the GT-1 and GT-2 trackways, highlighted with the black colour.





Isochirotherium gardettae ichnosp. nov

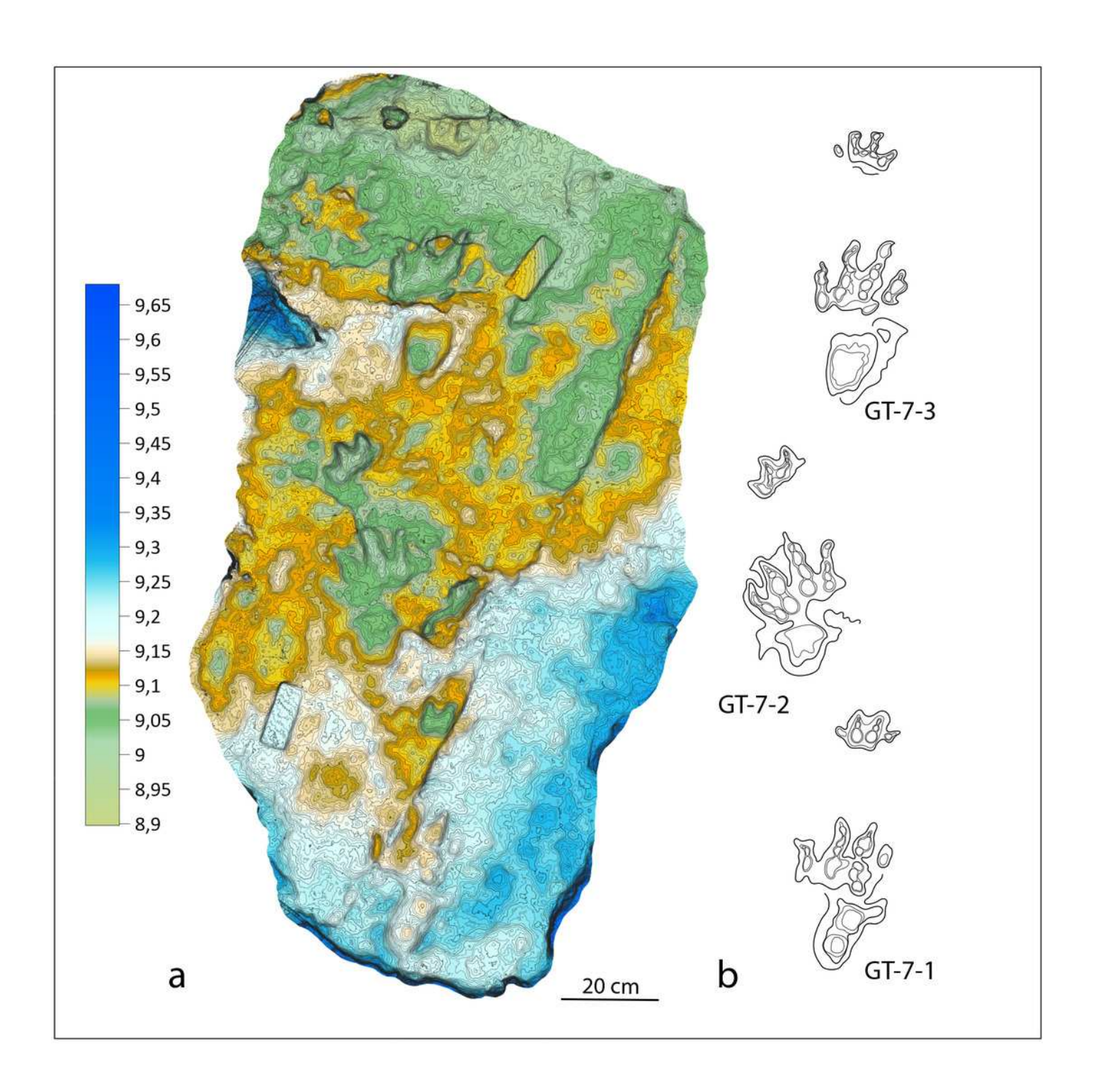
**Fig. 4** – *Isochirotherium gardettae* ichnosp. nov. The GT-7 trackway, made of three consecutive manus-pes couples, is here highlighted by the red chalk and preserved in the upper track-bearing surface. Scale bar: 13 cm.





*Isochirotherium gardettae* ichnosp. nov. Colour-coded and contour line image of the GT-7 trackway

**Fig. 5** – a) *Isochirotherium gardettae* ichnosp. nov. Colour-coded and contour line image of the GT-7 trackway; b) Interpretative drawing of the GT-7 trackway.

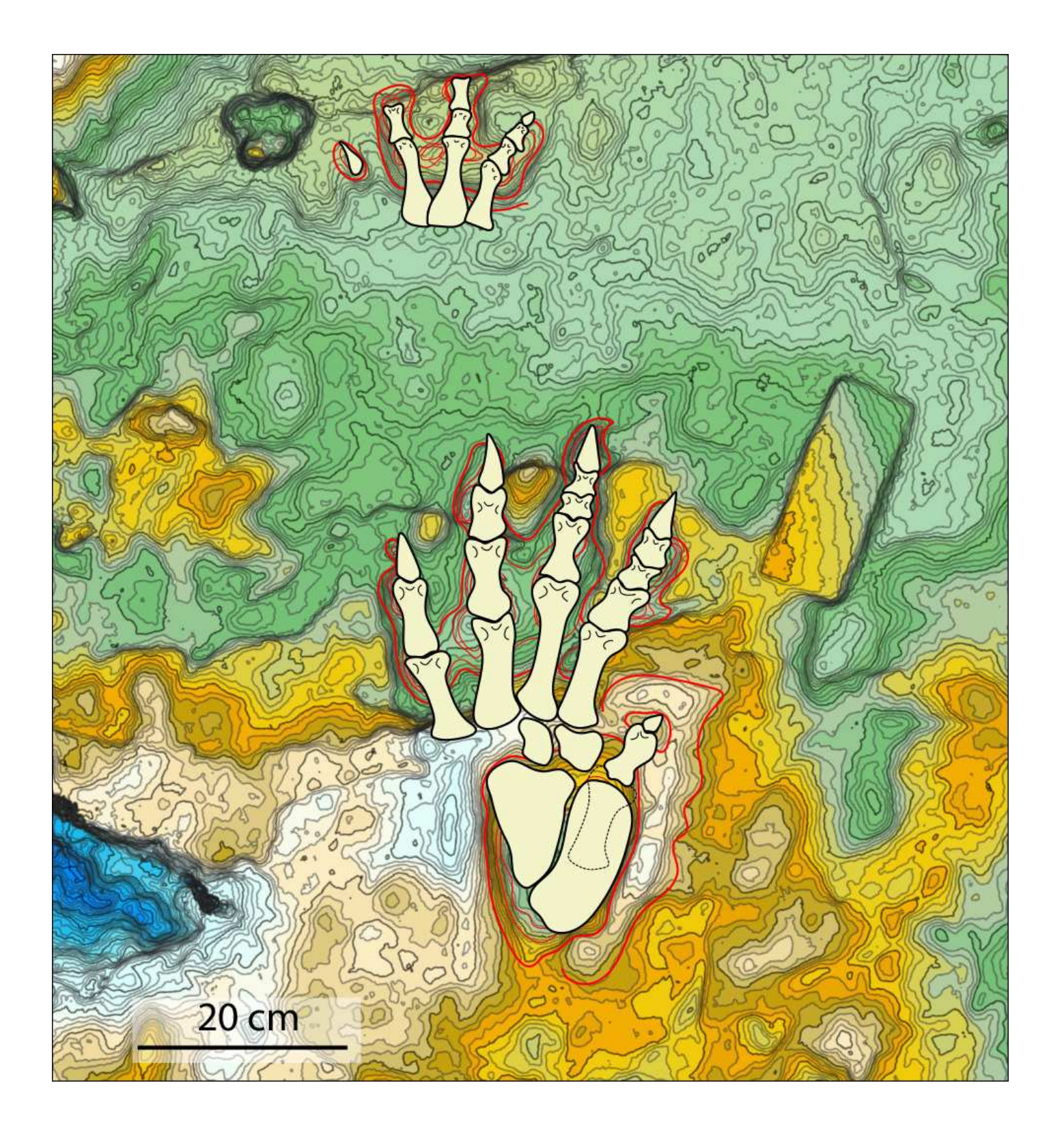




Reconstruction of the trackmaker's fore- and hind limbs, based on the 3D model and its interpretative drawing

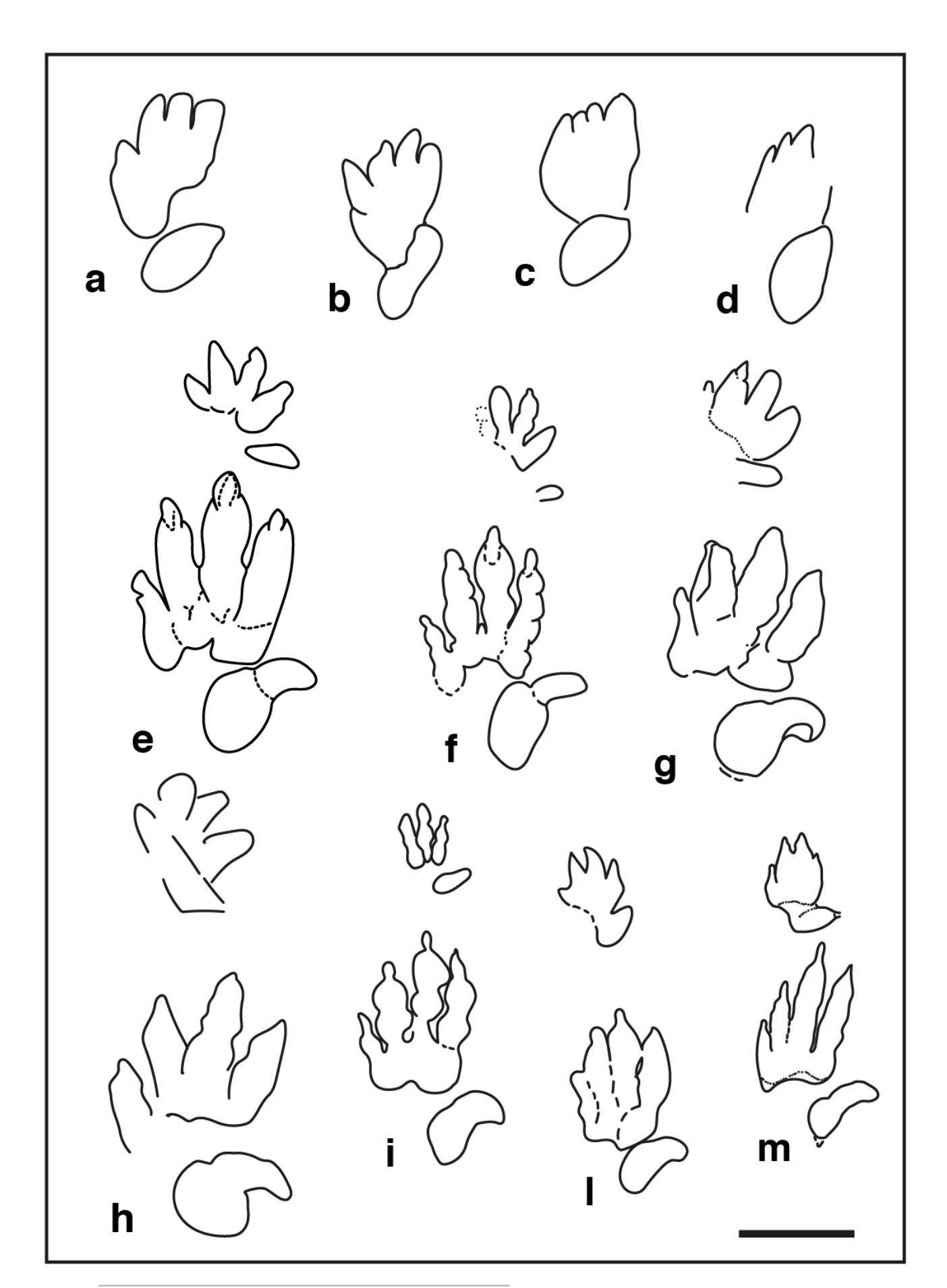
**Fig. 6** – Reconstruction of the trackmaker's fore- and hind limbs, based on the 3D model and its interpretative drawing. Dashed lines define the metatarsal of digit V held lifted off the ground during locomotion.





Pentadactyl tracks from the Lower and Middle Triassic, assigned to the ichnogenus *Chirotherium* and their comparison with the studied tracks of the Gardetta ichnosite

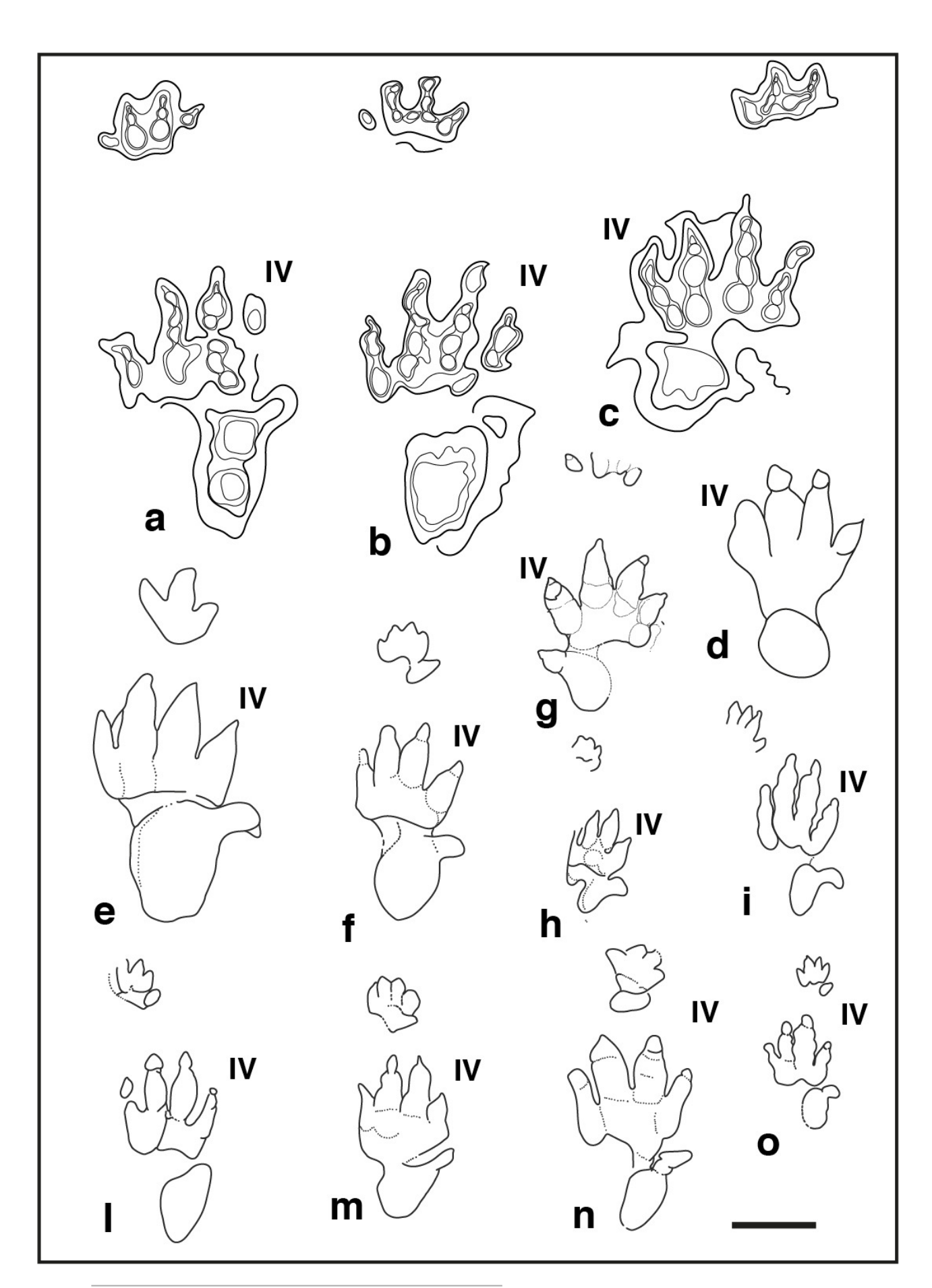
**Fig. 7** - Pentadactyl tracks from the Lower and Middle Triassic, assigned to the ichnogenus *Chirotherium* and their comparison with the studied tracks of the Gardetta ichnosite. (a) GT-1-3. (b) GT-2-3. (c) GT-2-8. d) GT-2-6; (e) and (f) *Chirotherium barthiii* pes manus sets from type surface of the "Thüringischer Chirotheriensandstein", Hildburghausen, Germany. (g) *Chrotherium barthiii* pes manus set from the Holbrook Member of the Moenkopi Formation (Middle Triassic), southwest of Cameron, northern Arizona. (h) *Chirotherium vorbachi* pes manus set from the Lower Triassic of Aura an der Saale, Germany (i), *Chirotherium sickleri* "Thüringischer Chirotheriensandstein", Germany. (I) and (m) *Chirotherium sickleri* pes manus sets from the Wupatki Member of the Moenkopi Formation (Lower Triassic), Meteor Crater, Arizona. Scale bar 10 cm.





Pentadactyl tracks from the Lower and Middle Triassic, assigned to the ichnogenus Isochirotherium and their comparison with the studied tracks of the Gardetta ichnosite

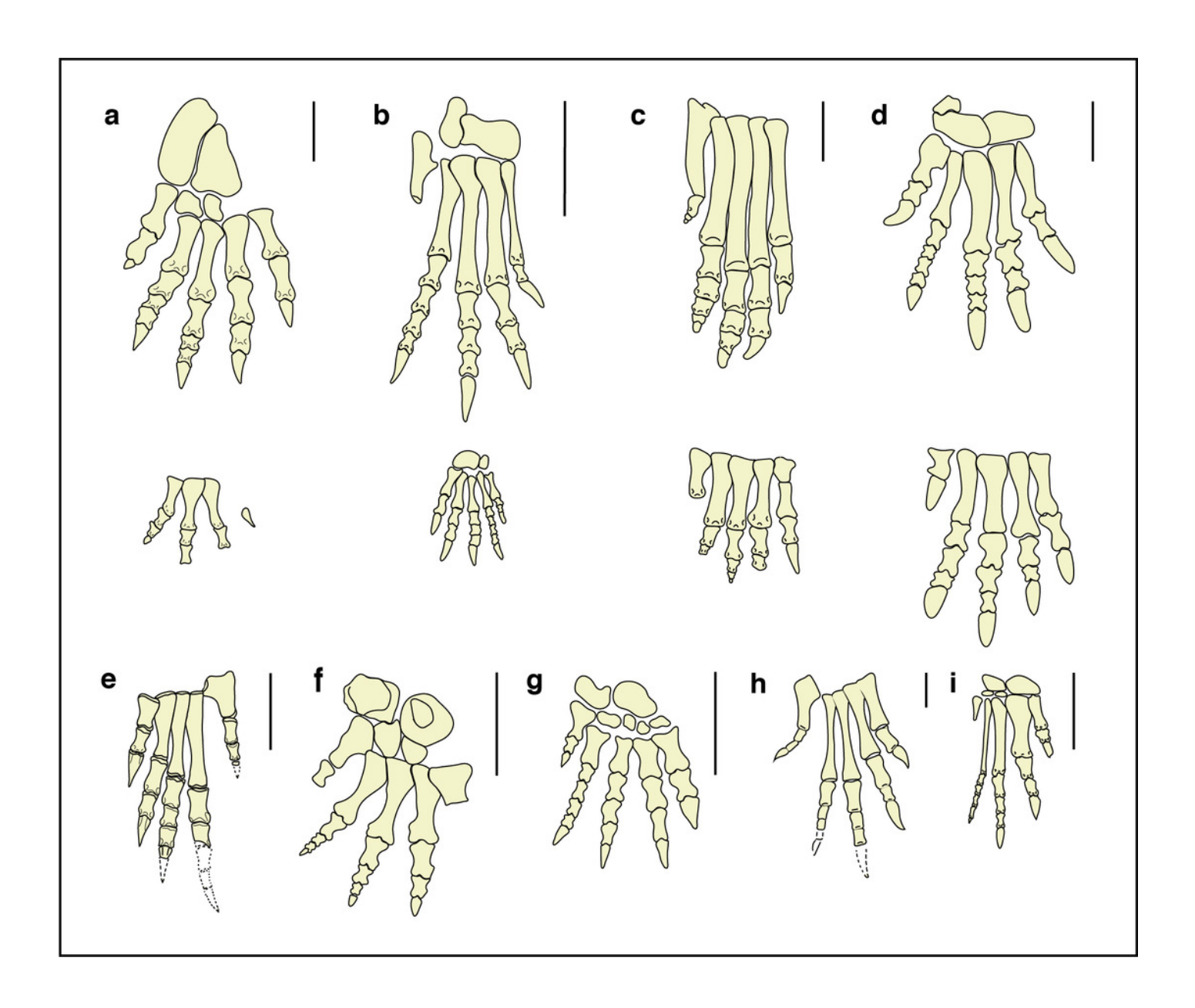
Fig. 8 - Pentadactyl tracks from the Lower and Middle Triassic, assigned to the ichnogenus Isochirotherium and their comparison with the studied tracks of the Gardetta ichnosite (a), (b), (c) Pes manus sets of the GT-7 trackway. (d) GT-3 isolated pes imprints of the lower track surface. (e) Isochirotherium herculis pes manus set from the "Thüringischer Chirotheriensandstein" (Lower Triassic), Germany. (f) Isochirotherium marshalli pes manus set from the Holbrook Member of the Moenkopi Formation (Middle Triassic), Penzance, Northern Arizona. (g) Isochirotherium inferni manus pes set from the Middle Triassic (late Anisian) of Adige Valley, Bolzano, Italy. (h) Isochirotherium coltoni pes manus set from the Wupatki Member of the Moenkopi Formation (Lower Triassic), Meteor Crater, Arizona. (i) Isochirotherium Iomasi pes manus set from the Middle Triassic (Anisian) of Cheshire, Great Britain. (I) *Isochirotherium coureli* pes manus set from the Middle Triassic (Anisian-Ladinian) of the Massif Central, France. (m) *Isochirotherium hessbergense* pes manus set from the "Thüringischer Chirotheriensandstein" (Lower Triassic), Germany. (n) Isochirotherium demathieui pes manus set from the Middle Triassic of Mont d'Or Lyonnais, France. (o) Isochirotherium soergeli pes manus set from the "Thüringischer Chirotheriensandstein" (Lower Triassic), Germany. Scale bar 10 cm.





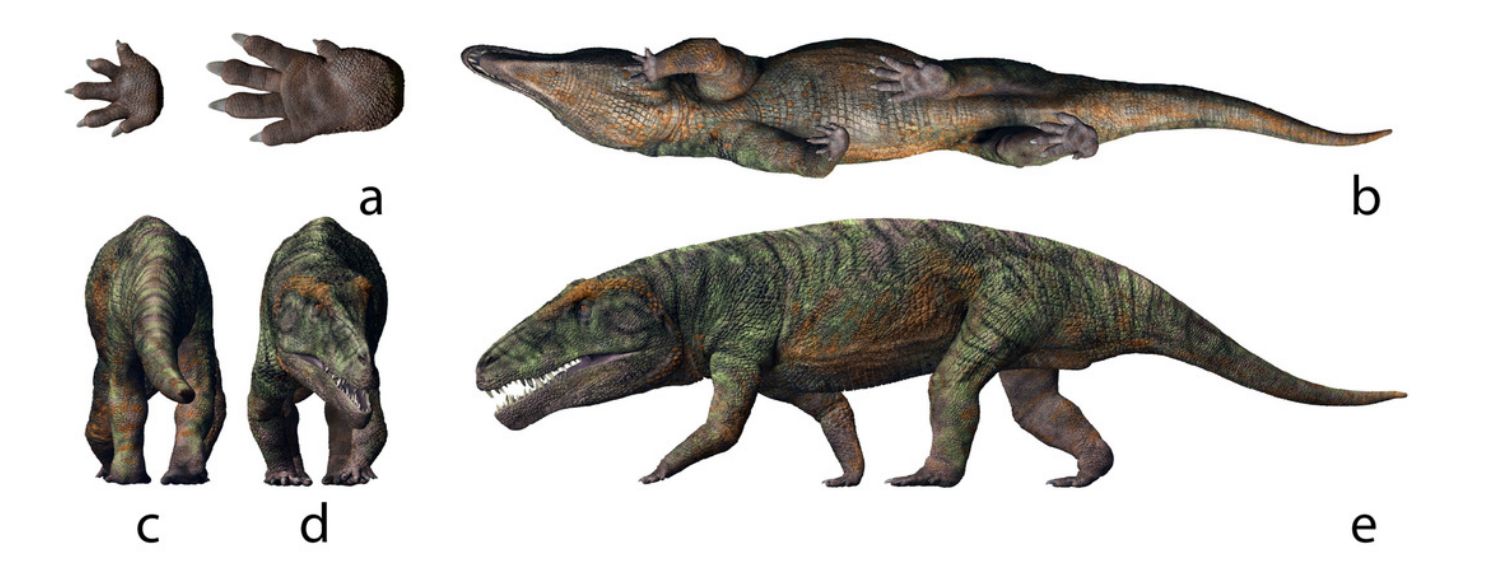
Fore- and hind-limb skeletons of Triassic archosauriforms and of the *Isochirotherium* gardettae trackmaker

**Fig. 9** - Fore- and hind-limb skeletons of Triassic archosauriforms and of the *Isochirotherium* gardettae trackmaker. Reconstructed right pes and manus skeletons of (a) The *Isochirotherium gardettae* trackmaker in anterior/dorsal view. (b) *Postosuchus kirkpatricki* Chatterjee 1985, USA, Norian. (c) *Postosuchus alisonae*, Peyer et al. 2008, USA, Norian. (d) *Lotosaurus adentus* Zhang, 1975, China, Ladinian. (e) *Proterosuchus fergusi* Broom 1903, South Africa, Induan-?early Olenekian. (f) *Erythrosuchus africanus* Broom 1905, South Africa, early Anisian. (g) *Shansisuchus shansisuchus* Young 1964, China, late Anisian. (h) *Euparkeria capensis* Broom, 1913, South Africa, Anisian. (i) *Chanaresuchus bonapartei* Romer, 1971, Argentina, Ladinian. Scale bars: a), b), c), d), f) g) = 10 cm; e), h) and i) = 1 cm.



Life appearance of the non-archosaurian archosauriform (?Erythrosuchid) the most suitable producer of *Isochirotherium gardettae* 

**Fig. 10** – Life appearance of the non-archosaurian archosauriform (?Erythrosuchid) the most suitable producer of *Isochirotherium gardettae*. Simplified reconstruction of fore and hind autopodials in bottom (a) view. Complete life reconstruction in bottom (b), back (c), frontal (d) and lateral view (e) of the trackmaker. The gait and fore- and hind limbs were reconstructed according to the pattern and morphologies of GT-7 trackway (artwork by the Italian artist Fabio Manucci). See the supplementary video to get a more complete view of the reconstruction.



Paleogeographic distribution of Early Triassic archosauriform footprints and body fossil localities across Pangea

**Fig. 11** - Paleogeographic distribution of Early Triassic archosauriform footprints (yellow stars) and body fossil localities across Pangea. Black square = indeterminate archosauromorphs, red circles = non-archosauriform archosauromorphs, blue stars = archosauriforms. The palaeolatitude estimate for the southern Briançonnais domain is 11.8 N in the Olenekian (250 Ma), confirming that archosauriforms were distributed also at low latitudes, in the tropical humid climatic belt. ImagePaleomap for 250 Ma downloaded from Fossilworks using data from the Paleobiology Database (Alroy, 2003). Redrawn and modified from Bernardi et al., 2015 and Benton (2018).

